

DENSITY FUNCTIONAL THEORY STUDY OF ALDOL
CONDENSATION BETWEEN FURFURAL AND 2-
BUTANONE OVER MAGNESIUM OXIDE

Miss Wilasinee Heebnak



A Thesis Submitted in Partial Fulfillment of the Requirements
for the Degree of Master of Science in Chemical Technology
Department of Chemical Technology
Faculty of Science
Chulalongkorn University
Academic Year 2019
Copyright of Chulalongkorn University

การศึกษาทฤษฎีฟังก์ชันเชิงความหนาแน่นของแอลคอลลคอนเดนเซชันระหว่างเฟอร์พิวรัลกับ 2-
บิวทาโนนบน แมกนีเซียมออกไซด์



วิทยานิพนธ์นี้เป็นส่วนหนึ่งของการศึกษาตามหลักสูตรปริญญาวิทยาศาสตรมหาบัณฑิต
สาขาวิชาเคมีเทคนิค ภาควิชาเคมีเทคนิค
คณะวิทยาศาสตร์ จุฬาลงกรณ์มหาวิทยาลัย
ปีการศึกษา 2562
ลิขสิทธิ์ของจุฬาลงกรณ์มหาวิทยาลัย

วชิลาสิณี หีบขนาด : การศึกษาทฤษฎีฟังก์ชันเชิงความหนาแน่นของแอลคอลลอนเดนเซชันระหว่างเฟอร์ฟูรัลกับ 2-บิวทานอนบน แมกนีเซียมออกไซด์ . (DENSITY FUNCTIONAL THEORY STUDY OF ALDOL CONDENSATION BETWEEN FURFURAL AND 2-BUTANONE OVER MAGNESIUM OXIDE) อ.ที่ปรึกษาหลัก : ดร.มนัสวี สุทธิพงษ์

ความเข้าใจข้อมูลเชิงลึกของกลไกและอุณหพลศาสตร์ในการเกิดปฏิกิริยาการควบแน่นอัลคอลลอนเดนเซชันมีความสำคัญต่อการเปลี่ยนเชิงเร่งปฏิกิริยาของสารประกอบออกซิเจนจากชีวมวลเป็นเชื้อเพลิงไฮโดรคาร์บอน งานวิจัยนี้ศึกษาปฏิกิริยาการควบแน่นอัลคอลลอนเดนเซชันของเฟอร์ฟูรัลและ 2-บิวทานอนบนแมกนีเซียมออกไซด์โดยใช้การคำนวณฟังก์ชันเชิงความหนาแน่น การคำนวณรูปแบบพลังงานประกอบด้วยสามขั้นตอนหลักได้แก่ ขั้นตอนที่ 1 การเกิดอินเลตของ 2-บิวทานอน ขั้นตอนที่ 2 การเกิดพันธะคาร์บอน-คาร์บอน และขั้นตอนที่ 3 การกำจัดน้ำออกจากโมเลกุลเพื่อเกิดผลิตภัณฑ์สุดท้าย ผลการคำนวณพบว่าขั้นตอนการเกิดอินเลตของ 2-บิวทานอนเป็นขั้นตอนกำหนดอัตราการเกิดปฏิกิริยาโดยการเกิดอินเลตของ 2-บิวทานอนด้านเมทิลมีระดับพลังงานที่ต่ำกว่า อย่างไรก็ตามการเกิดปฏิกิริยาผ่านอินเลตของ 2-บิวทานอนด้านเมทิลีน (โครงสร้างโซ่กิ่งเป็นผลิตภัณฑ์) เกิดได้ง่ายกว่าด้านเมทิล (โครงสร้างโซ่ตรงเป็นผลิตภัณฑ์) เนื่องจากมีค่าพลังงานก่อกัมมันต์ที่ต่ำกว่า ผลการคำนวณฟังก์ชันเชิงความหนาแน่นที่ได้เป็นพื้นฐานความเข้าใจในกลไกการเกิดปฏิกิริยาบนตัวเร่งปฏิกิริยาชนิดเบสและอาจใช้เป็นแนวทางในการศึกษาปฏิกิริยาการควบแน่นอัลคอลลอนเดนเซชันบนตัวเร่งปฏิกิริยาชนิดออกไซด์ผสม



จุฬาลงกรณ์มหาวิทยาลัย
CHULALONGKORN UNIVERSITY

สาขาวิชา เคมีเทคนิค
ปีการศึกษา 2562

ลายมือชื่อนิสิต
ลายมือชื่อ อ.ที่ปรึกษาหลัก

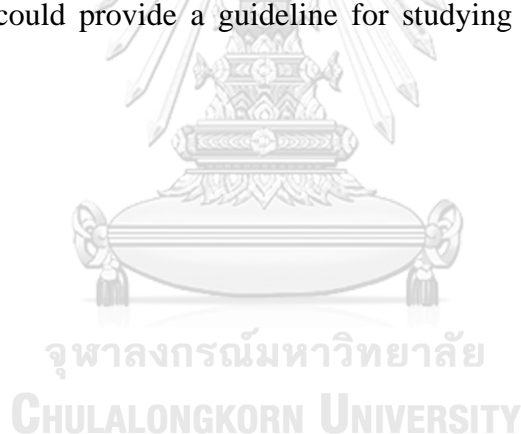
6072151623 : MAJOR CHEMICAL TECHNOLOGY

KEYWORD

D:

Wilasinee Heebnak : DENSITY FUNCTIONAL THEORY STUDY OF ALDOL CONDENSATION BETWEEN FURFURAL AND 2-BUTANONE OVER MAGNESIUM OXIDE . Advisor: Dr. Manaswee Suttipong

Understanding of mechanistic and thermodynamic insights of the aldol condensation reaction is crucial to efficient catalytic conversion of biomass-derived oxygenates to fuel-range hydrocarbons. In this study, the aldol condensation of furfural and 2-butanone on magnesium oxide (MgO) catalyst was investigated using density functional theory (DFT) calculations. Energy profiles were computed for elementary steps, including Step 1: Formation of 2-butanone enolate, Step 2: Enolate addition at the carbonyl group of adsorbed furfural, and Step 3: Dehydration to form the condensation product. The DFT results showed that the enolization of 2-butanone was the rate-determining step. The methyl enolate can bind to MgO surface with low energy. The methylene enolate route (generating branched product) was favored compared to the methyl enolate route (yielding linear product) due to lower activation energy. The DFT results offer a base-catalyzed basis for understanding reaction mechanism and could provide a guideline for studying reaction on mixed oxide catalyst.



Field of Study: Chemical Technology

Student's Signature

Academic Year: 2019

Advisor's Signature

Year:

.....

ACKNOWLEDGEMENTS

I would like to express the deepest appreciation to my advisor, Dr. Manaswee Suttipong, and Associate Professor Vudhichai Parasuk, who have the attitude and the substance of genius: they continually and convincingly in regard to teaching. Without their guidance and persistent help this dissertation would not have been possible.

I would like to acknowledge Assoc. Prof. Dr. Prasert Reubroychaoen, Assoc. Prof. Dr. Chawalit Ngamcharussrivichai and Dr. Pussana Hirunsit for serving as chairman and member of the dissertation committee, respectively.

I would like to acknowledge Mr. Pavee Pongsajanukul and Mr. Thanawit Kuamit who like my brothers for guiding and supporting everything in my work.

I would like to thank the Center of Excellence in Computational Chemistry (CECC), at Department of Chemistry, Faculty of Science, Chulalongkorn University and National Electronics and Computer Technology Center (NECTEC) for computing facility, and I would like to thank Center of Excellence on Petrochemical and Materials Technology (PETROMAT) for financial support.

I would also like to thank staff and the members of the Department of Chemical technology for their kind support.

Finally, I would like to express my deep gratitude to my family and my boyfriend for their support and love.

จุฬาลงกรณ์มหาวิทยาลัย
CHULALONGKORN UNIVERSITY

Wilasinee Heebnak

TABLE OF CONTENTS

	Page
.....	iii
ABSTRACT (THAI)	iii
.....	iv
ABSTRACT (ENGLISH)	iv
ACKNOWLEDGEMENTS	v
TABLE OF CONTENTS	vi
Chapter 1 Introduction	8
1.1 Introduction	8
1.2 Objective.....	9
Chapter 2 Literature review and Theoretical Background	10
2.1 Furfural	13
2.2 2-Butanone	14
2.3 Aldol condensation.....	14
2.4 Magnesium oxide catalyst	16
2.5 Computational theory	17
2.5.1 The Schrodinger equation	17
2.5.2 Hartree-Fock (HF) approximation.....	18
2.5.3 Density functional theory (DFT).....	19
Chapter 3 Research design and Computational details	20
3.1 Simulated system.....	20
3.2 Proposed mechanism of aldol condensation between 2-butanone and furfural on MgO surface	21
3.3 Computational details	23
Chapter 4 Results and discussions	24
4.1 Geometry Optimization	24
4.2 Transition state (TS)	24

4.3 Energy profile.....	26
4.4 Bond distance.....	31
4.5 Thermodynamic properties.....	33
Chapter 5 Conclusion and Recommendation	35
5.1 Conclusion.....	35
5.2 Recommendation.....	35
REFERENCES	27
VITA.....	30



Chapter 1 Introduction

1.1 Introduction

Over the past decade, as driven by the problems of limited fossil fuels and their impact on the environment, great efforts have been devoted to the efficient synthesis of fuels and chemicals from renewable biomass [1]. C–C bond formation via heterogeneous catalyzed aldol condensation of biomass-derived platform molecules [2], such as acetone, furfural, or 5-hydroxymethylfurfural (HMF), is a promising approach to construct larger organic molecules in order to yield valuable liquid hydrocarbons [3]. The aldol condensation of symmetric ketone compound gives only one product such as acetone while asymmetric ketone gives two different products such as 2-butanone and levulinic acid. Recently, the aldol condensation of furfural with 2-butanone has been studied by using Mg-Al layered double hydroxide derived mixed oxide catalysts to produce C9 oxygenates, including straight (C9S) and branched (C9B) components. The proposed reaction pathways are illustrated in **Figure 1**. The C9S and the C9B can react again with themselves or furfural or 2-butanone, obtaining C13-C18 compounds. These compounds can be further converted into biofuels via hydrodeoxygenation [4]. Importantly, experimental observations indicate that the C9B aldol product was strongly favored over the C9S one, more likely dependent on which enolate forms (i.e., methyl and methylene groups) of 2-butanone react with furfural. While branched product from methylene route can be used to produce jet fuel, linear product from methyl route can be used to produce bio-diesel.

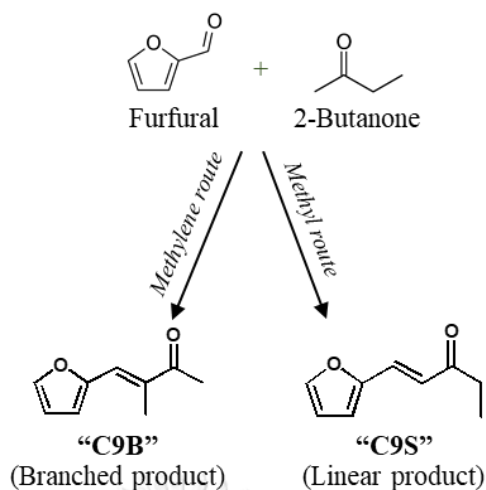


Figure 1 The proposed reaction pathways of aldol condensation between furfural and 2-butanone.

In this study, density functional theory (DFT) calculations are performed to unravel the mechanism of the aldol condensation between furfural and 2-butanone on MgO (100) surface. The corresponding activation energies are obtained. Adsorption energies of each reactant and product are also calculated, which is crucial not only for predicting the performance of the MgO catalyst, but also complementing experimental investigations.

1.2 Objectives

1. To study reaction mechanism for the aldol condensation reaction between furfural and 2-butanone over MgO surface
2. To calculate energy profiles of the reaction paths including

Step 1: Enolization of 2-butanone to generate 2-butanone enolate

Step 2: C-C coupling between furfural and 2-butanone enolate

Step 3: Dehydration to form the condensation product

Chapter 2 Literature review and Theoretical Background

Aldol condensation is a valuable C–C bond formation reaction that provides an efficient way of increasing the carbon chain length of molecules containing a carbonyl group[5], such as aldehydes, ketones, carboxylic acids and esters. There are various researches studying reaction of aldol condensation to produce biofuel as follows

Kikhtyanin et al. [6] elucidated the properties of zeolites of different structural type and their catalytic performance in the aldol condensation of furfural and acetone. The results showed that the acidic zeolites possessed rather good activity in aldol condensation of furfural and acetone. The highest conversion of furfural was observed when using wide pore zeolites with a three-dimensional crystalline framework. The results suggested that Brønsted acid sites were essential in the transformation. During the reaction, the activity of the investigated zeolites decreased due to the formation of carbonaceous deposits inside their micropores.

Levulinic acid (LA) is one of the most promising chemicals derived from biomass, used as feedstock for further transformations. Liang et al. [7] investigated the aldol condensation of furfural with LA in the aqueous phase on MgO and ZnO. β - and δ -furfurylidenelevulinic acids (FDLA) were produced as two isomeric products in the aldol condensation reaction. The results showed that MgO and ZnO were active and selective catalysts with respect to aqueous phase aldol condensation. MgO gave a high selectivity towards δ -FDLA due to the water-tolerant basicity, while ZnO was highly selective towards β -FDLA, indicative of an acid-catalyzed aldol reaction mechanism. In addition, nano-ZnO with a relatively high surface area gave rise to enhanced yields of β -FDLA.

Faba et al. [8] studied the catalytic aqueous-phase aldol condensation of acetone and furfural on mixed oxides (Mg-Zr, Mg-Al and Ca-Zr, with different basic sites distribution). Catalysts with the highest concentration of basic sites were the most active and selective for the C13 fraction, whereas molar ratios of 1:1 yielded the highest selectivity for C13 fraction. Concerning to reaction mechanism, cis isomers were the first ones formed, whereas trans isomers were the most abundant at higher reaction times. The mechanism of the aldol reaction was proposed as presented in **Figure 2**. The

results suggested that the kinetic of products was dependence on the concentration of reactant, and the formation of the enolate was the rate-determining step. The proposed mechanism was used to design the calculation mechanism in Section 3.3.

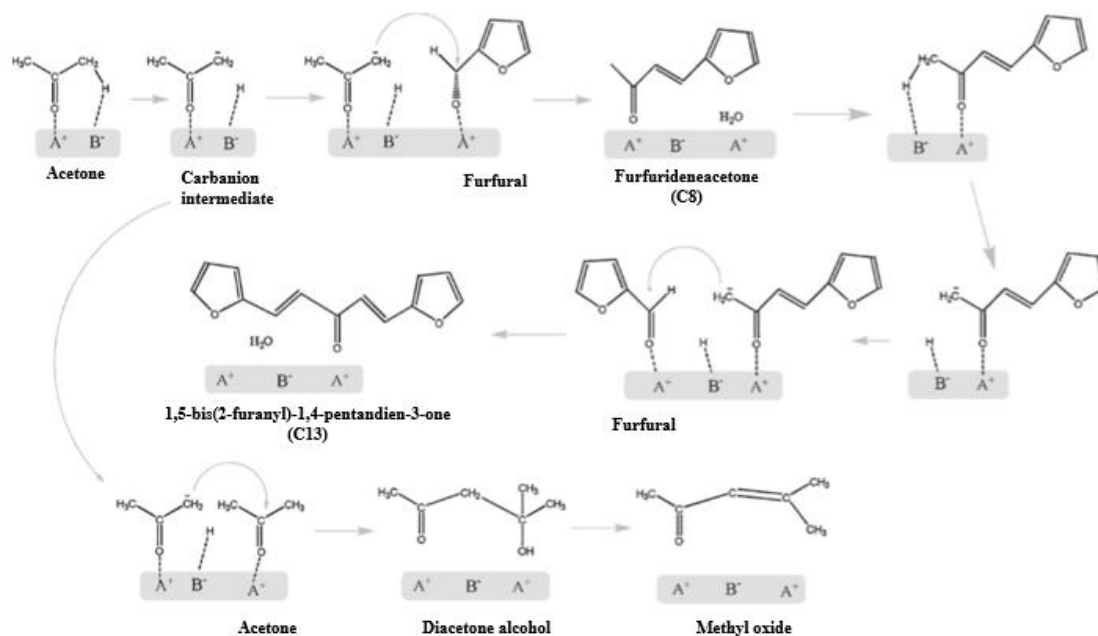


Figure 2 Surface process for the aldol condensation of acetone with furfural [8].

In recent decades, molecular simulation techniques centered on density functional theory (DFT) calculations have quickly become a powerful research and technology development instrument. In particular, the knowledge and theory gained from DFT-based techniques have effectively transformed understanding of the fundamental surface science, catalysis, and materials science. Using DFT calculations, Zhao et al. [9] identified three primary reaction steps in the aldol condensation of 5-hydroxymethylfurfural (HMF) with LA: (1) deprotonation of LA to generate LA ions, (2) LA ions addition at hydroxymethyl site of HMF, and (3) internal dehydration to form the condensation product. The reaction pathway through the C5 of LA formed a linear product that was favored with respect to both energy and configuration in all three elementary reaction steps. This was qualitatively consistent with the phenomenon observed in experiment where the linear form was a main product. All of DFT calculations throughout this work were carried out using the Gaussian 09 software package. The B3LYP with hybrid exchange functional were used for all geometry optimization and frequency calculations. Additional calculations were performed using

the M06-2X, TPSS27 and MP228 in order to compare the results from various functionals. The M06-2X functional has a very good response under dispersion forces, improving one of the biggest deficiencies in DFT methods. Reaction mechanism for self- and cross-aldol condensation of cycloketones, including cyclopentanone (C5) and cyclohexanone (C6), over ZrO_2 catalyst was studied by Wan et al. [10], experimentally and computationally. The results revealed that the conversion of C5 was much higher than C6 in their self-aldol condensation reactions. In the cross-aldol condensation, where C5 and C6 were both present, the conversions of both C5 and C6 were greatly enhanced. DFT simulation results suggested that both C5 and C6 can readily adsorb on ZrO_2 surface due to their high binding energy. The adsorbed C6 was hard to be activated because of its higher energy barriers of the keto-enol tautomerization and C–C bond formation. Accordingly, C12 product was significantly less, compared to others. In the cross-aldol condensation of C5 and C6, a metastable intermediate of a seven-membered ring was identified which dramatically decreased the energy barrier of the reaction, leading to the high yield of C11. **Figure 3** shows the reaction energy profiles, obtained from DFT calculations, for the self- and cross-aldol condensation of C5 and C6 on ZrO_2 .

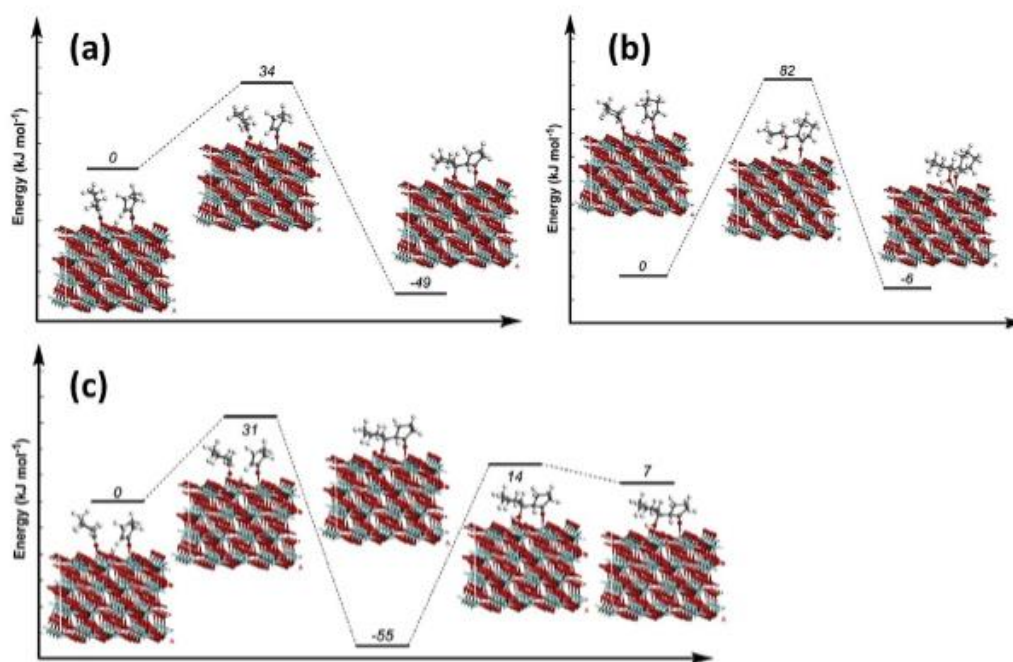


Figure 3 Energy profile for self- and cross-aldol condensation of C5 and C6 on ZrO_2 [10].

In this work, DFT was studied the mechanism between furfural and 2-butanone over MgO for producing biofuel precursors. Thus, the theoretical background includes details of furfural, 2-butanone, aldol condensation and density functional theory.

2.1 Furfural

Furfural (IUPAC name: Furan-2-carbaldehyde) is an aldehyde with the formula C_4H_3OCHO that is furan with hydrogen at position 2 substituted by formyl group. The structure of furfural [11] is illustrated in the **Figure 4**. Furfural is a colorless liquid oil, whereas commercial samples are often brown. Furfural is one of the furan derivatives formed from the hemicellulose of lignocellulosics biomass [12]. It can be produced by hydrolysis and dehydration of xylose, a pentose sugar which often found in hemicellulose fraction of lignocellulosics biomass [13]. Furfural performs in the same reaction as aldehydes and aromatic compound it has two main functional groups (aldehyde and olefin groups). Thus, it can used for various reactions such as acylation, reduction, acetylation, decarboxylation, oxidation, and aldol condensation. Furfural has been extensively used in industrial chemical. Furfural can be converted to various derivative forms that have been widely applied as bio-plastics, biofuel, transportation fuels, resins [14], enhancers for food and drinks etc.

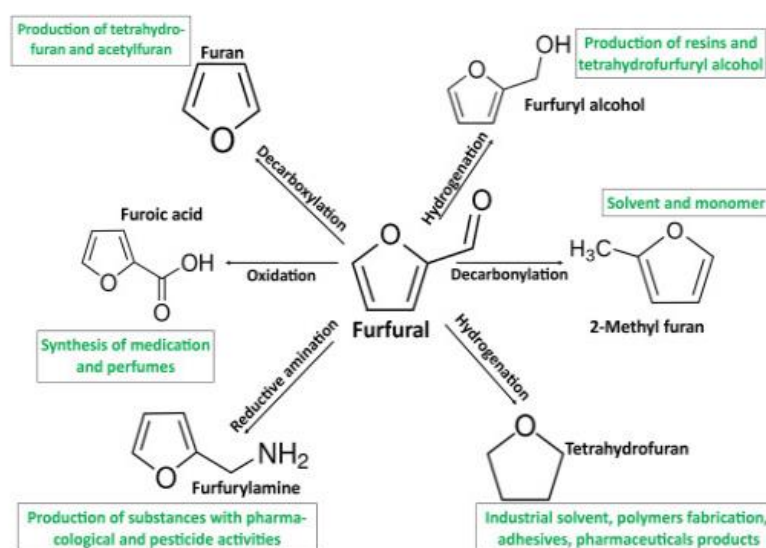


Figure 4 The structure of furfural and its derivative forms [11].

2.2 2-Butanone

2-butanone or methyl ethyl ketone is a ketone compound with the chemical formula $\text{CH}_3\text{C}(\text{O})\text{CH}_2\text{CH}_3$. It is a colorless liquid ketone. 2-Butanone can produce by nature and produced in industrial. Synthesis of 2-butanone from glucose [15] that is synthesized by fermentation and hydration under suitable temperature and pressure (**Figure 5**) [16]. It performs in the similar reaction as acetone or ketone compound; nevertheless, higher boiling point and has a significantly slower evaporation rate. 2-butanone is an important chemical of wide application in industrial. It can be used in various reaction for example aldol condensation, polymerization [17].

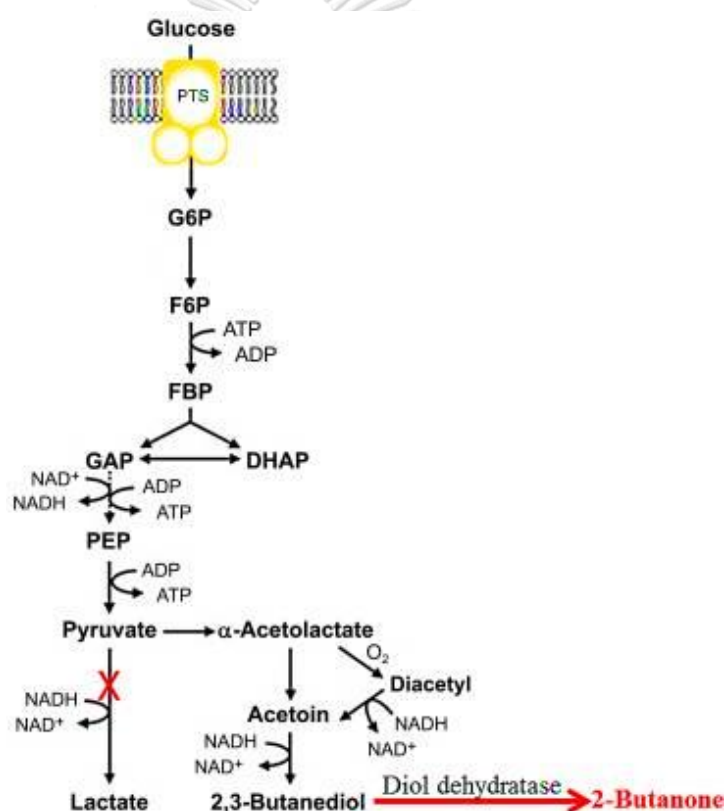


Figure 5 Synthesis of 2-butanone from glucose [16].

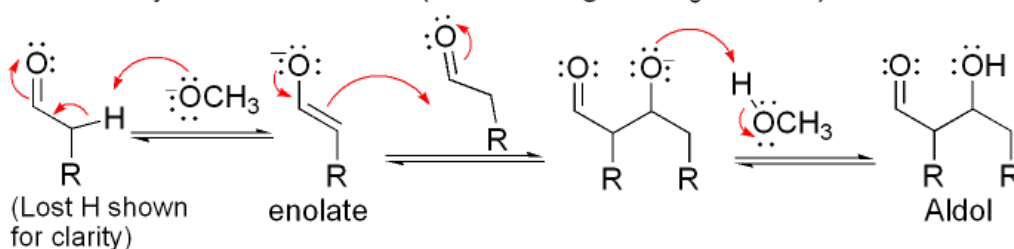
2.3 Aldol condensation

Aldol condensation is an important addition reaction in organic synthesis between aldehyde or ketone [18]. An enol or enolate reacts with a carbonyl group of another aldehyde or ketone (to form carbon-carbon bond) to form hydroxyaldehyde or

hydroxyketone, followed by dehydration to produce a longer carbon chain compound [19]. Aldol condensation between aldehyde and ketone compound that react at the alpha carbon of ketone. Thus, the number of reaction pathways and product up to the number of alpha carbons of ketone. Symmetric ketone that has only one alpha carbon so, the aldol condensation of symmetric ketone gives one reaction pathways and product. Because asymmetric ketone has different two alpha carbon, the aldol condensation of asymmetric ketone can give two different reaction pathways and products.

The aldol condensation can react via homogeneous catalyst or heterogeneous catalyst by both acid and base. Base catalyzed are forming carbon-carbon bonds via an intermediate enolate [20], [21] while acid catalyzed are forming carbon-carbon bonds via an intermediate enol. The mechanism of base catalyzed and acid catalyzed are summarized in **Figure 6** and **Figure 7**.

Base catalyzed aldol reaction (shown using $^-OCH_3$ as base)



Base catalyzed dehydration (sometimes written as a single step)

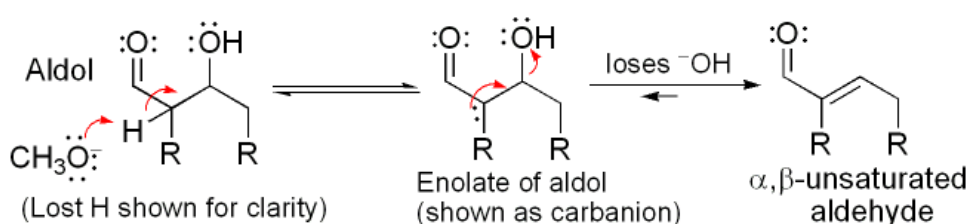


Figure 6 Mechanism of aldol condensation (base catalyzed) [22].

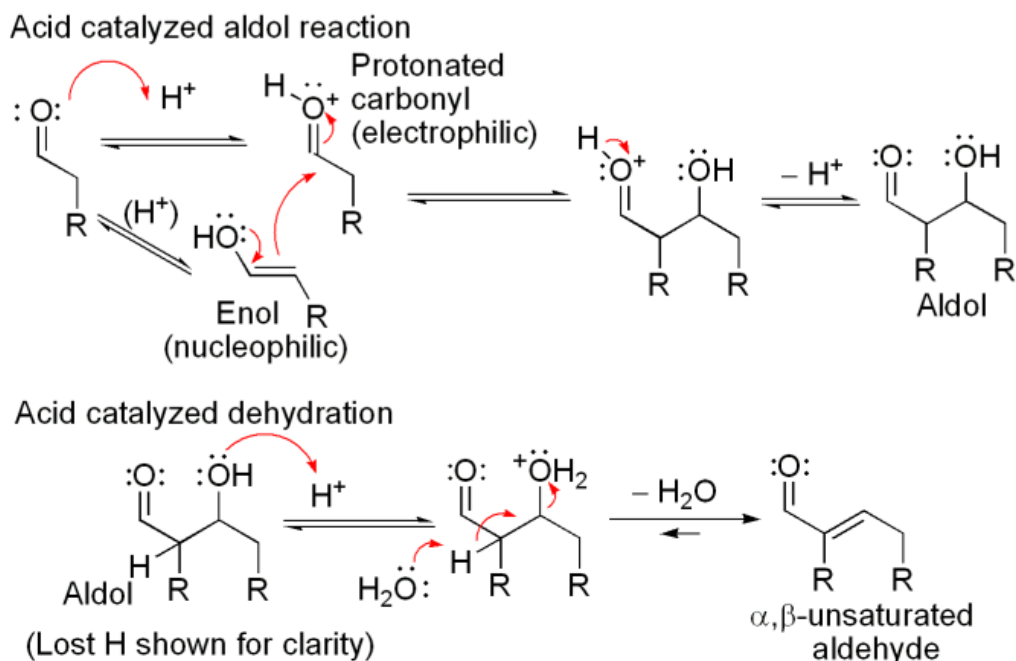


Figure 7 Mechanism of aldol condensation (acid catalyzed) [22].

The mechanism of base catalyzed aldol condensation. First, a base reaction. Base catalyst abstracts the hydrogen atom at the α -C to convert an enol form intermediate which then attacks the carbonyl group of the aldehyde and generate intermediate alkoxide. Finally, base catalyst will be protonated and dehydrated to form aldol product. While the mechanism of acid catalyzed aldol condensation is based on the formation of enol species. The mechanism of acid catalyzed aldol condensation is initiated by the lone pair electron of oxygen at carbonyl attacks the carbonyl group of the aldehyde. This step generates the carbocation or enol form. The enol form attacks the carbonyl group of the aldehyde to form product and dehydrated to form aldol product. Thus, the aldol condensation can be reacting via base catalyzed and acid catalyzed. In this work, the base catalyst is focused as it is suitable for aldol condensation step [8].

2.4 Magnesium oxide catalyst

Magnesium oxide (MgO) catalyst is a white solid that include magnesium and oxygen atom. **(Figure 8)** Magnesium oxide catalyst is a heterogeneous catalysis that show the phase of catalyst differs from phase of product and reactant [23]. Magnesium oxide catalyst is more stable at high temperature. The properties of magnesium oxide

catalyst are high-surface area, additive and promoter of many kind of chemical reaction. It can use for high thermal conductivity and low electrical conductivity. Thus, it was used as a base-catalyzed in many applications for many reactions such as aldol condensation, reforming, hydrodesulfurization.

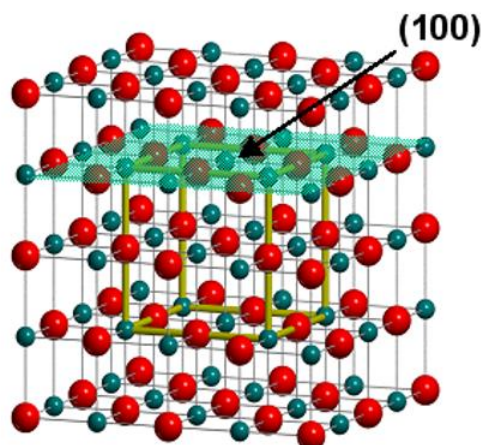


Figure 8 Structure of MgO catalyst [24].

2.5 Computational theory

Density functional theory (DFT) is a computational quantum chemistry that was established by laws of physics [25], used in chemistry, physics and materials science to examine the electron density of many system. Using density functional theory, the properties of electron density can be determined by functional [26].

2.5.1 The Schrodinger equation

In the field of quantum theory studies Erwin Schrödinger proposed the different ways to solve system problems which studied the behavior of electron and nucleus. The Schrodinger equation is measurement operator that transformed from Hamiltonian mechanics. The energy of system depends on Hamiltonian operator that can be written as an equation of Eigenequation [27].

The Schrodinger equation is

$$H\Psi = E \Psi$$

Where H is Hamiltonian operator, Ψ is the wave function and E is the energy of system

The general of Hamiltonian operator that explain by

$$H = -\sum_i \frac{\hbar^2}{2m} \nabla_i^2 - \sum_{i,l} \frac{Z_l e^2}{|r_i - R_l|} + \frac{1}{2} \sum_{i,j} \frac{e^2}{|r_i - r_j|} - \sum_l \frac{\hbar^2}{2M} \nabla_l^2 + \frac{1}{2} \sum_{l,j} \frac{Z_l Z_j e^2}{|R_l - R_j|}$$

Hamiltonian in the form of sum of energy are shown in the right of equation that consist of the first term, sum of kinetic energy from the movement of electrons [28]. The second term, sum of potential energy from the force of attraction between electron and nuclei. The third term, sum of potential energy from the force of attraction between electron and electron. The fourth term, sum of kinetic energy from the movement of nuclei. And the fifth term, sum of potential energy from the force of attraction between nuclei and nuclei respectively. But the approximation is based on the fact of the system that electron nuclei much slower than electron due to their masses [29]. Thus, Hamiltonian operator is reduced to solve the equation that is

$$H = -\sum_i \frac{\hbar^2}{2m} \nabla_i^2 - \sum_{i,l} \frac{Z_l e^2}{|r_i - R_l|} + \frac{1}{2} \sum_{i,j} \frac{e^2}{|r_i - r_j|}$$

To find the answer of the equation that can be extent with the estimation method by Hartree-Fock. They suggest that the wave function of electron group can be written from determinant of matrix.

2.5.2 Hartree-Fock (HF) approximation

In the computational chemistry, the Hartree-Fock (HF) approximation is a method for determination of wave function and energy in state [30]. The HF approximation used to variate principle to find the minimum $E \Psi$ which is product of N spin orbital.

The Hartree-Fock (HF) can be obtained by many electrons wave function

$$\Psi_{\alpha_1, \dots, \alpha_N(q_1, \dots, q_N)}^\alpha = \frac{1}{\sqrt{N!}} \begin{vmatrix} \phi_{\alpha_1}(q_1) & \dots & \phi_{\alpha_1}(q_N) \\ \vdots & & \vdots \\ \phi_{\alpha_N}(q_1) & \dots & \phi_{\alpha_N}(q_N) \end{vmatrix}$$

However, when compare with the experimental results found that Hartree-fock methods still higher than the experimental. This method is not suitable for many electron groups. Thus, HF cannot apply in the large system. Trying to find the answer of the equation in the system used density functional theory that is based on density rather than orbitals in HF.

2.5.3 Density functional theory (DFT)

Hohenburg and Kohn who stated a theorem that electron density is very useful [31]. The theorem of Hohenburg and Kohn asserts the density of system that determines the total ground state energy of electron. They suggested the accuracy of DFT can find the energy and properties of electron density of system which is the function of position

The energy of DFT can be written by

$$E_{DFT} = E_{NN} + E_T + E_V + E_{coulomb} + E_{xx}$$

Where E_{NN} is the energy of the repulsion between nuclear and nuclei, E_T is the kinetic energy of electron, E_V is the energy of attraction between electron and nuclei, $E_{coulomb}$ is coulomb repulsion of electron-electron, and E_{xx} is the ecchange eenergy of non-classical electron-electron.

Chapter 3 Research design and Computational details

3.1 Simulated system

Aldehyde and ketone can react via aldol condensation to produce biofuel. This work focusses on furfural and 2-butanone as aldehyde and ketone molecule. Thus, furfural has been reacting with 2-butanone via aldol condensation over MgO surface. The simulated system includes 2-butanone, furfural and MgO.

2-Butanone includes 1 atom of oxygen, 4 atoms of carbon and 8 atoms of hydrogen, shown in the Figure 3.1. The structure of 2-butanone was used in cis-form. The structure of 2-butanone was constructed using GaussView.

Furfural include 2 atoms of oxygen, 5 atoms of carbon and 4 atoms of hydrogen, shown in the **Figure 8**. The structure of 2-butanone was constructed using GaussView.

Cluster models were constructed to represent two layers of MgO (100) surface using Material studio 6.1 and GaussView. MgO includes 35 atoms of magnesium, 35 atoms of oxygen (**Figure 9**). MgO unit clusters were used to model two layers of MgO and two layers of MgO cluster was utilized to simulate MgO (100) (**Figure 10**). The reaction was simulated on MgO (100) surface.

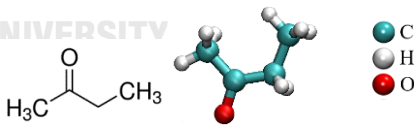
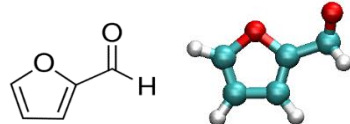
Name	Chemical formula	Structure
(a) 2-Butanone	C_4H_8O	
(b) Furfural	$C_5H_8O_2$	

Figure 9 The structure of furfural and 2-butanone.

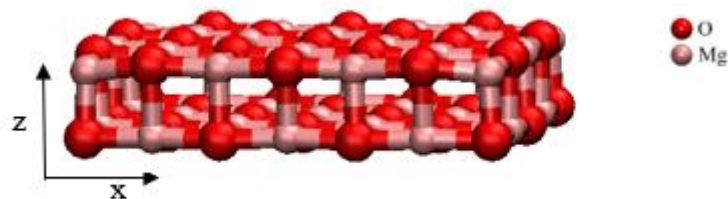


Figure 10 The structure of MgO (100) surface, size $2 \times 2 \times 1$ in x, y, and z.

3.2 Proposed mechanism of aldol condensation between 2-butanone and furfural on MgO surface

Aldol condensation is the one of the most common organic reaction in which carbonyl compounds were coupled, forming C-C bond and dehydration for produce a longer carbon chain compound. Aldol condensation reaction react with α -hydrogen of ketone. The mechanism was designed via Reference [8], that is the reaction between acetone and furfural. Acetone has symmetry structure thus the reaction occurs though α -hydrogen only one way. 2-butanone has asymmetry structure, thus the reaction occurs though different two α -hydrogen, the reaction has two difference routes. The reaction occurs though α -hydrogen at methylene that show the branched product. On the other hand, the reaction occurs though α -hydrogen at methyl that show the branched product.

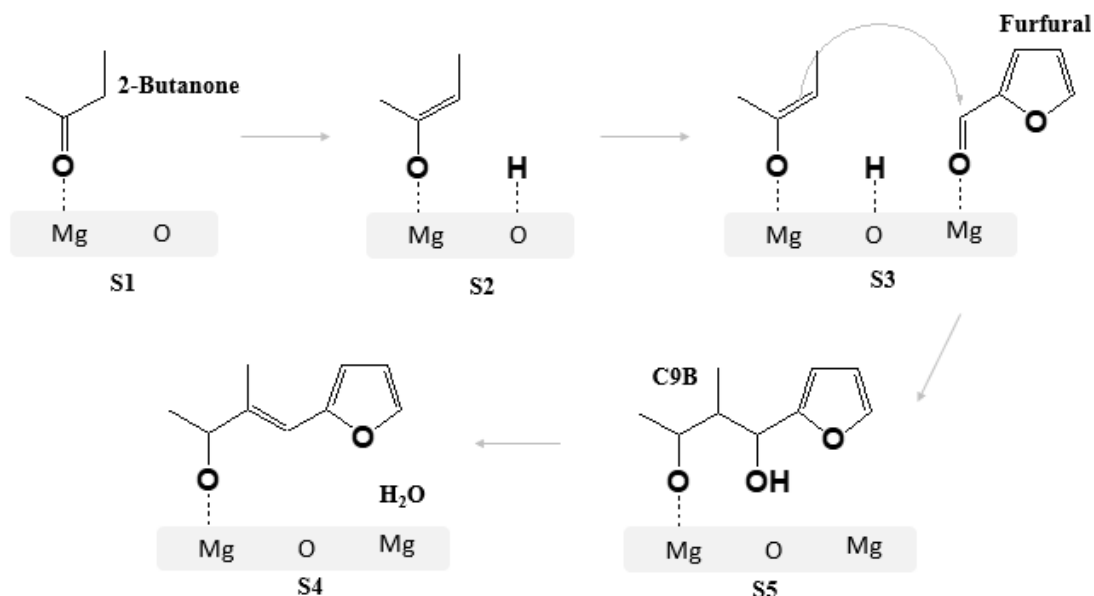
Figure 11 shows the proposed mechanism, including 3 elementary steps including:

Step1: The enolization of 2- butanone. The α -hydrogen bond with O atom of MgO to convert enolate form (see S1-S2 in **Figure 10**).

Step2: C-C coupling of 2-butanone enolate and furfural. 2-butanone enolate attacks with carbonyl of furfural to produce intermediate (see S3-S4 in **Figure 10**).

Step3: Dehydration of product. The final step is dehydration to produce final product (see S4-S5 in **Figure 10**).

(a) Methylene route (Branched product)



(b) Methyl route (Linear product)

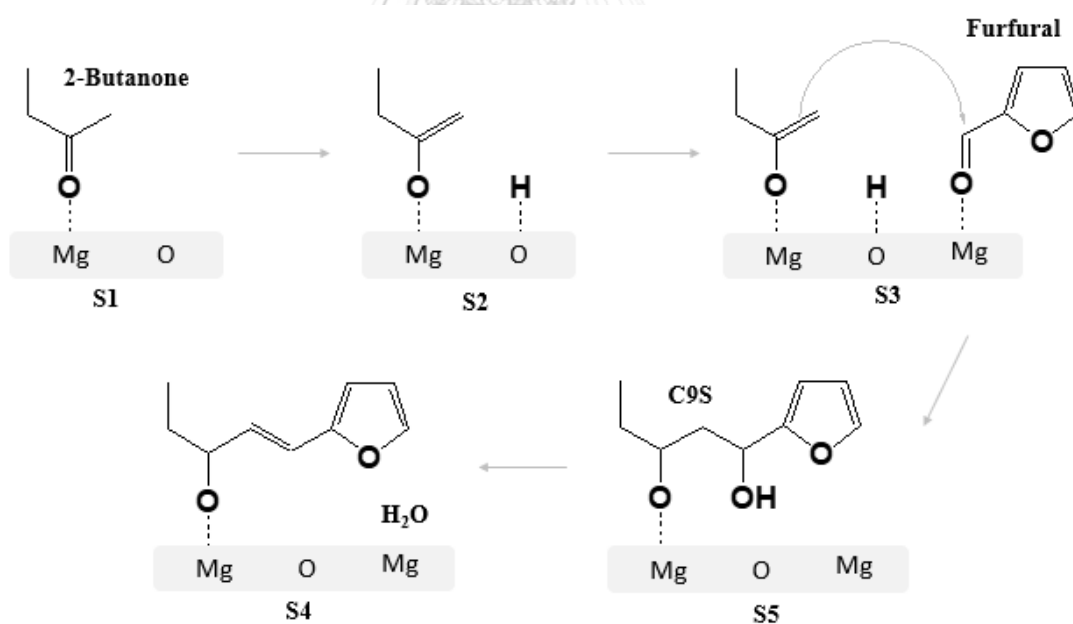


Figure 11 The proposed mechanism of aldol condensation between furfural and 2-butanone on MgO surface including: methylene route (a) and methyl route (b) (S1= 2-Butanone absorbed on MgO, S2= Enolate form on MgO, S3= C-C coupling between 2-butanone enolate and furfural, S4= Product from C-C coupling and S5= Final product).

3.3 Computational details

The atom representing the bottom two layers were frozen their positions. All molecule and transition states were constructed using GaussView optimized with the Gaussian 09 package with M06-2X functional. 6-31G basic set was employed for optimization and was used to perform a single point energy reaction calculation as indicated[32]. All structure was fully optimized; frequency analyses were performed to ensure either a minimum was achieved. The transition state was calculated by optimization of each distance between the optimized reactants and products. The OPT=TS was visualized to confirm the expected motion of transition state structure. Then the calculations were optimized by energy barrier and transition state energy barrier for the local minimum. (The calculation shows in the appendix) The thermodynamic parameters of the reaction were calculated at 298 K and 1 atm. The energy barrier E were calculated by equations 1 and 2.

$$E = E_{total} - E_{MgO} - E_{2-Butanone} \text{ -----(1)}$$

$$E = E_{total} - E_{MgO} - E_{2-Butanone} - E_{Furfural} \text{ -----(2)}$$

When E_{total} is energy of complex,

E_{MgO} , is energy of 2 layers MgO surface.

$E_{2-butanone}$ is energy of 2-butanone molecule.

and $E_{Furfural}$ is energy of furfural molecule.

Chapter 4 Results and discussions

The results include geometry optimization, transition State (TS), energy profile, bond distance and thermodynamic properties.

4.1 Geometry Optimization

The energy minimization (also called energy optimization) is the process to find an arrangement in space of a collection of atoms. The binding energy were calculated by energy minimization of energy optimization in the equation 3.3. The binding energy shows in **Table 1**. The binding energy of methylene route (giving branched route) is slightly higher than that of methyl route (giving linear product). From the energy optimization, it was found that the values of energy calculated for both routes were slightly different.

Table 1 Binding energy of each step (kcal/mol).

	S1	S2	S3	S4	S5
Methylene route (Branched product)	-11.28	1.56	-430605.44	-430636.64	-382702.36
Methyl route (Linear product)	-15.41	-8.98	-430591.31	-430633.94	-382458.36

4.2 Transition state (TS)

The key to success for creates overall energy profile that must to find TS. The process to find TS is scanning energy that is related with the bond distance. TS S1-S2 is the transition state of enolization step and TS S3-S4 is the transition state of C-C coupling reaction. TS for S1 convert to S2 is varying O-H bond distance that vary initial to 1.0 Å (distance of O-H bond) and TS for S3 convert to S4 is varying C-C bond distance that vary initial to 1.54 Å (distance of C-C bond). The energy of scanning transition state for methylene route show in **Figure 12** (a and b). The energy of scanning transition state for methyl route is showed in **Figure 12** (c and d).

From the transition state energy S1-S2 of methylene route is 81.21 kcal/mol and 138.32 kcal/mol for methyl route. The transition state energy S3-S4 of methylene route is -430572.37 kcal/mol and -430578.75 kcal/mol for methyl route (detailed calculation of TS is present in reference). The highest energy is the transition state energy. From the transition state, S1-S2 is endothermic reaction and S3-S4 is exothermic reaction. Transition state energy S1-S2 of methylene route is lower than methyl route. The transition state energy S3-S4 of methylene route is higher than methyl route. Accordingly, the enolization reaction (S1-S2) of methylene route occurs easier than that of methyl route. On the other hand, addition reaction (S3-S4) of methyl route occurs easier than that of methylene route.

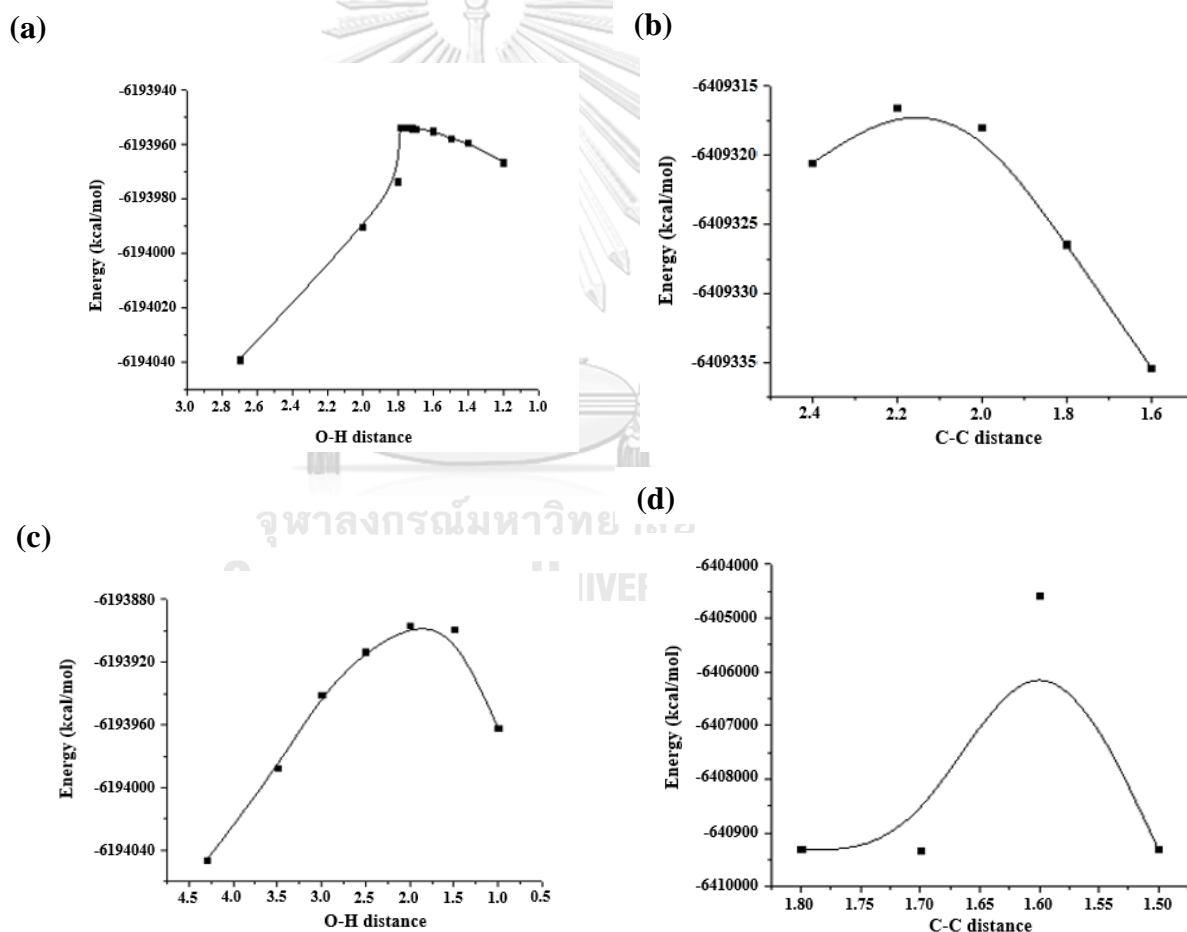


Figure 12 The energy of scanning transition state for methylene route ((a) TS for S1-S2 and (b) for S3-S4) and for methyl route (c) TS for S1-S2 and (d) for S3-S4).

4.3 Energy profile

4.3.1 Step 1: Enolization of 2-butanone to generate 2-butanone enolate

The first step of this aldol condensation is the enolization of 2-butanone which is an important step. The enolization is removal of a proton from the α -carbon to give the enolate. The energy profile is shown in the **Figure 13** and the corresponding structures are shown in **Figure 14** and **Figure 15**. The calculated barrier for the first enolization step starts with the absorption of 2-butanone molecule on MgO surface. From the optimization the abstraction of α -H on the 2-butanone leads to the formation of enolate yielding 1.56 kcal/mol for methylene route and -8.98 kcal/mol for methyl route. The activation energy of methylene enolization route is 52.95 kcal/mol and 153.73 kcal/mol for methyl enolization route. One can see from **Figure 13** that the methylene route is not only more favored but has a much smaller activation energy than that of linear route. This larger activation energy difference between two routes is probably due to bond distance between α -H of 2-butanone and O site of surface. Bond distance of the first enolization step is 2.7 Å for methylene route and 4.3 Å for methyl route that explain in 4.4. Hajek *et al.* [33] who studied mechanism of aldol condensation in UiO-66 and UiO-66-NH₂ metal organic framework. They reported similar observations that a proton jumps from the catalyst surface (Zr-oxo cluster) or called enolization show endothermic reaction.

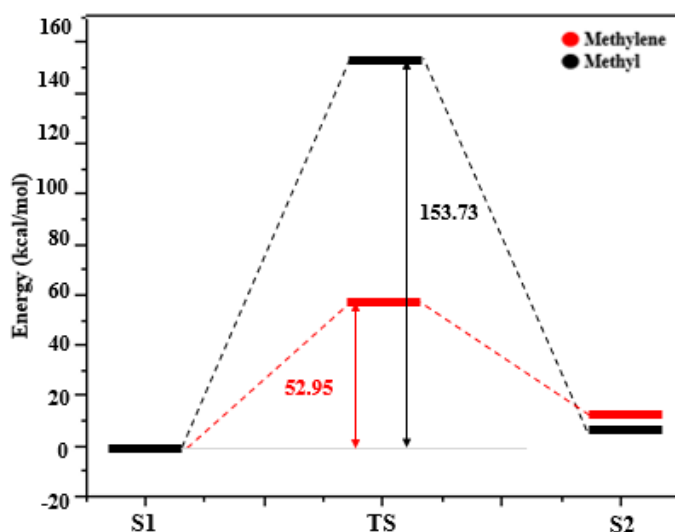


Figure 13 Energy profile of 2-butanone enolization to generate methylene (red line) and methyl (black line) enolates on MgO surface.

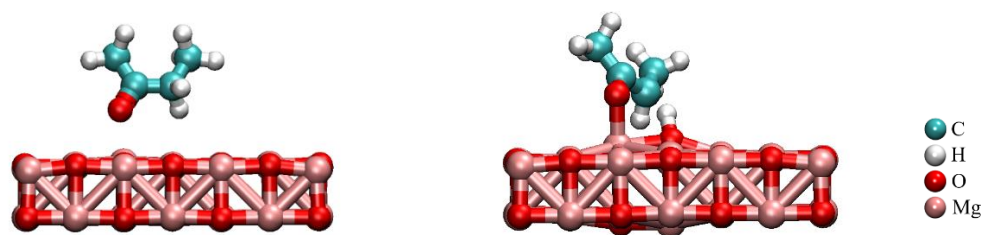


Figure 14 Structure of S1(left) and S2(right) (methylene route).

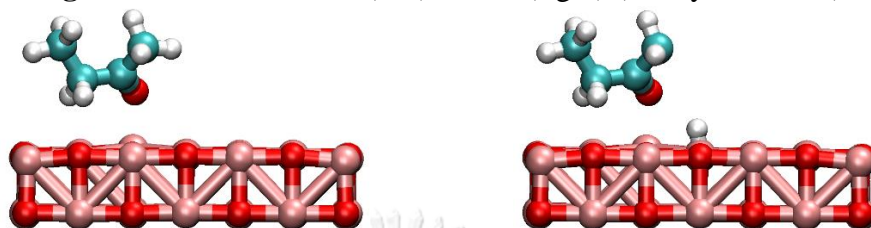


Figure 15 Structure of S1(left) and S2(right) (methyl route).

From the energy profile of enolization step, the energy level of enolate from of methyl route is lower than that of methylene route thus, the thermodynamic product in this step is methyl enolate and methyl enolate is more stable than methylene enolate. The activation energy of methylene route is lower than that of methyl route so, the kinetic product in this step is methylene enolate.

4.3.2 Step 2: C-C coupling between furfural and 2-butanone enolate

The resulting 2-butanone enolate can attack furfural via C-C coupling. C-C coupling reactions have been carried out on MgO catalysts (see **Figure 17** and **Figure 18**). These coupling reactions lead to the production of biofuel intermediates used in the next step. The coupling reactions between 2-butanone enolate from 4.3.1 and furfural, shown in **Figure 16** is identified for the methylene product route and the methyl product route. This step of reaction is endothermic in both routes. The result showed the activation energy of methylene route is 18.93 kcal/mol and 12.55 kcal/mol for methyl route. The energy barrier of transition state of methylene route is higher than methyl route and the energy in the step 4 of methyl more stable than methylene product. The activation energy of methylene route lower than methyl route. This probably due to the structure on the surface, 2-butanone enolate in methylene route has steric effect thus difficult for attack with carbonyl group of furfural. From the energy profile of this step that shows the C-C coupling or addition of methyl route easier to react than methylene route. The results are consistent with those obtained from Wan *et al.*, [10] who study the aldol

condensation of cycloketone on zirconia(ZrO_2) investigated the C-C coupling of cycloketone on ZrO_2 (111). The role of ZrO_2 is similar to MgO and the C-C coupling reaction is exothermic.

From the energy profile of C-C coupling step, the energy level of C-C coupling product of methyl route is lower than that of methylene route thus, the thermodynamic product in this step is methyl enolate and methyl enolate is more stable than methylene enolate. And activation energy of methyl route is lower than that of methylene route so, the kinetic product in this step is methyl enolate.

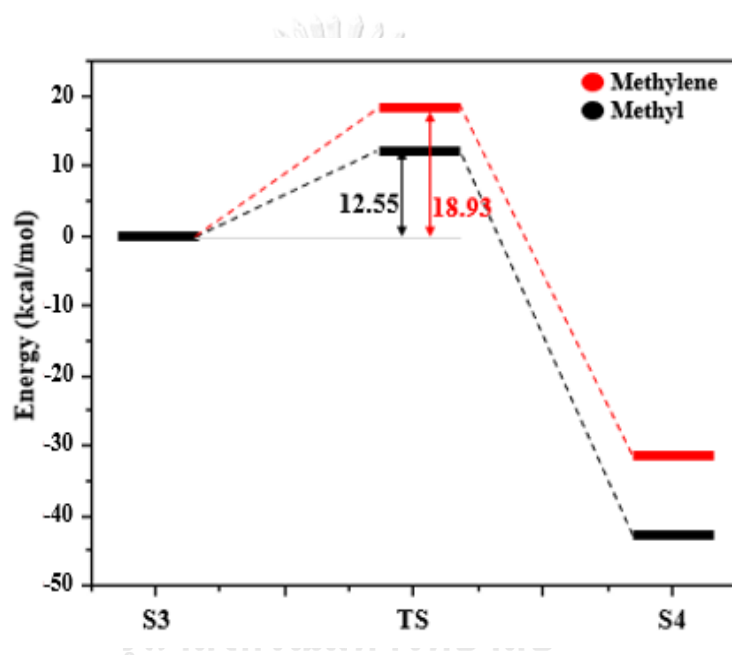


Figure 16 Energy profile of C-C coupling between 2-butanone enolate and furfural adsorbed on MgO surface (Methylene and methyl routes are shown in red and black line, respectively).

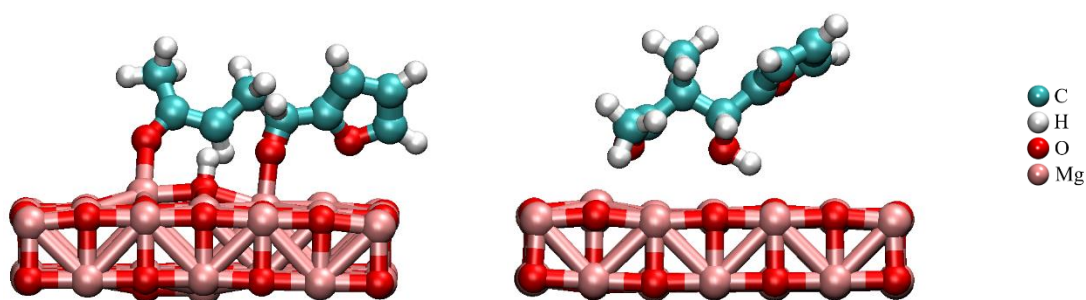


Figure 17 Structure of S3 and S4 (methylene route).

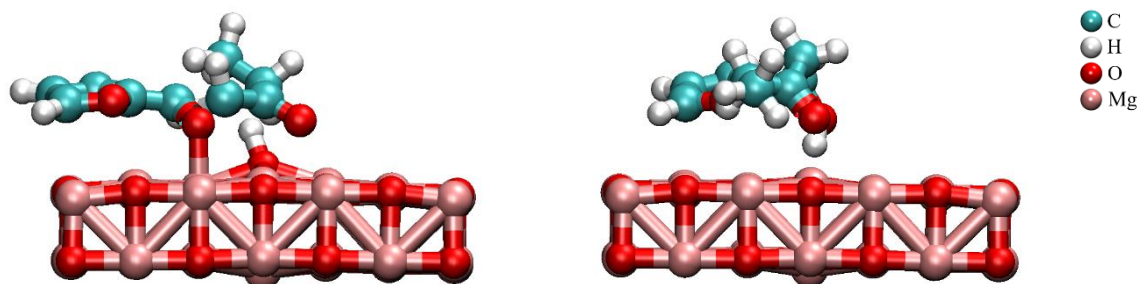


Figure 18 Structure of S3 and S4 (methyl route).

4.3.3 Step 3: Dehydration to form the condensation product

The final step is to form C=C double bond by dehydration to yield the final product.

One way to synthesize unsaturated compound is by dehydration of product, a process in which catalyst to lose water and form a double bond. The dehydration reaction of product to generate C=C bond proceeds by heating the alcohols in the presence of a catalyst, at high temperatures. Similar step in 4.3.1 and 4.3.2 also show the energy of both route the energy barrier of final product of methylene product is -382702.36 kcal/mol and -382458.36 kcal/mol in methyl product. (The structure of final product show in **Figure 19**) The final product of methylene route (Branched product) more stable than methyl route (Linear product). Zhao l. et al. [9] study the aldol condensation between HMF and levulinic acid in gas phase. Their result show linear product more favoured than branched product while in this work branched product more favoured than linear product. Thus their result report in different agreement with the this work of the aldol condensation between furfural and 2-butanone over MgO. Because the α -H abstraction of the ketone on a basic O site of MgO while in gas phase, no surface used to extract proton. Therefore, the reaction is based on steric effect.

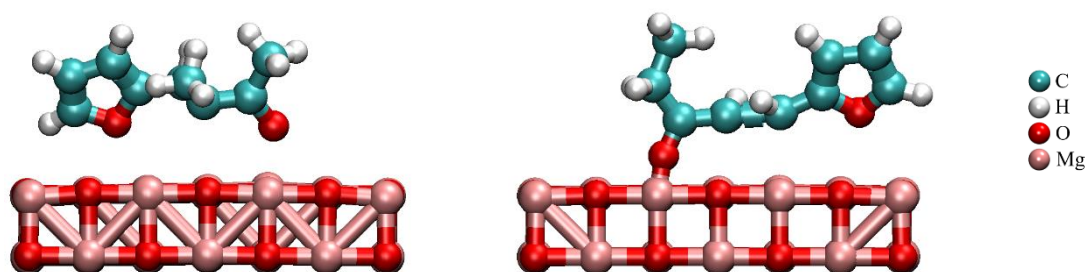


Figure 19 Structure of final product (methylene route: left, methyl route: right).

4.3.4 Full energy profile

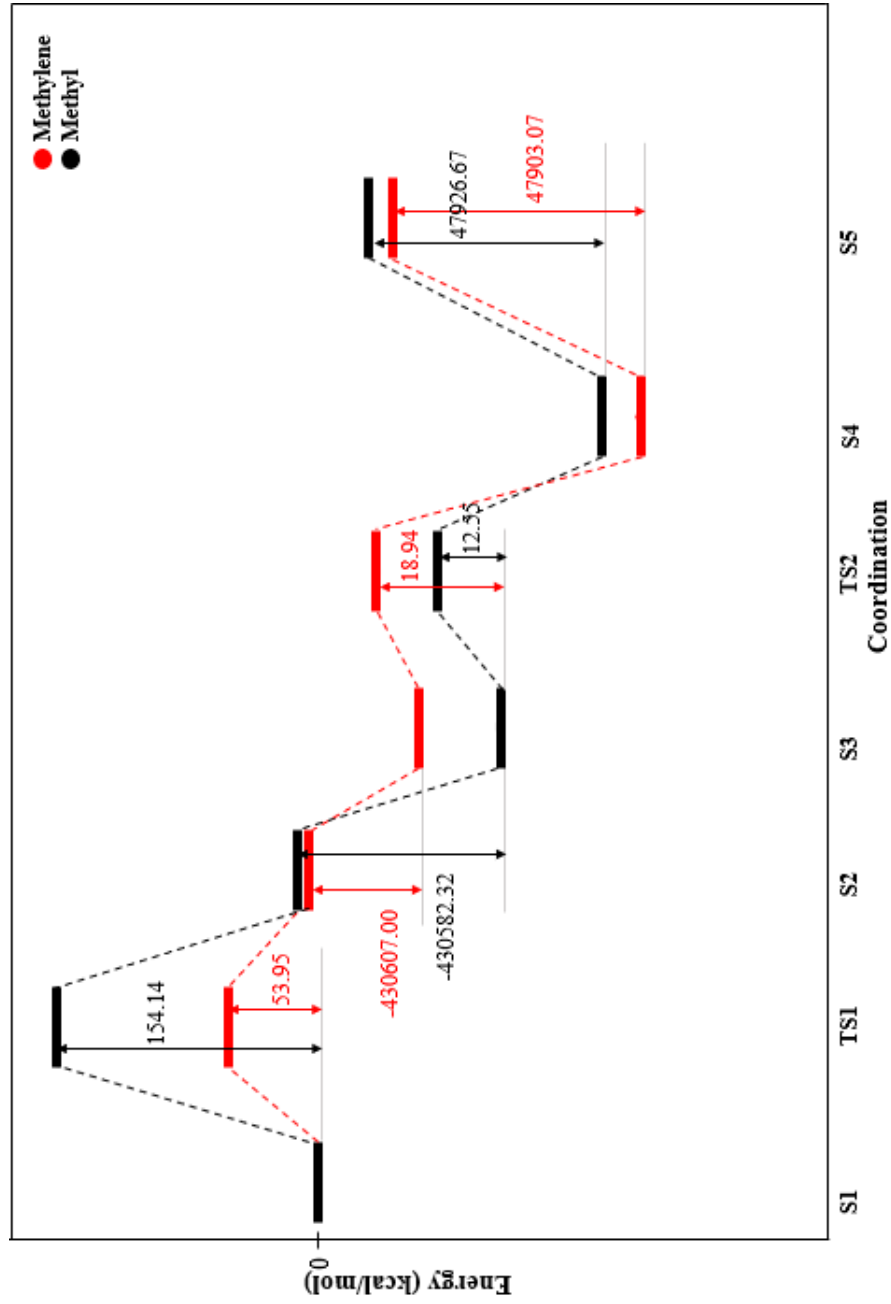


Figure 20 Energy profile of aldol condensation between furfural and 2-butanone on MgO.

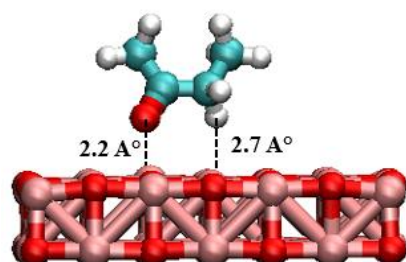
Overall energy profile (**Figure 20**), the energies of species in methylene route are still lower activation energy and the most of energy barrier each step are lower than methyl route. Except step3-4, the activation energy of methyl route is lower than methylene route. Even so, the energy different between methylene route and methyl route is only by 6.38 kcal/mol, which probably due to steric effect for C-C coupling reaction. Rate determining step is enolization because that show the highest activation energy in the overall energy profile. The result relates with Gao J. et al. [34] who study self-condensation of acetone over zinc oxide (ZnO). Their results are in line with this work that show enolization is the rate determining step. Moreover, the enolization step is endothermic and C-C coupling step is exothermic.

4.4 Bond distance

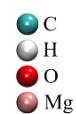
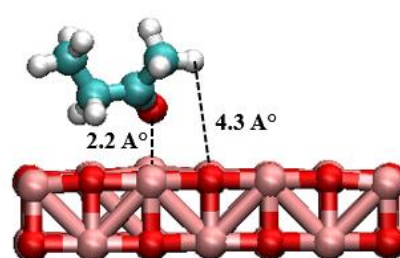
The bond length refers to the distance between atoms of molecule of two bonded atoms in an equilibrium position. The stronger the force of attraction in between the bonding atoms, the smaller is the length of the bond. From the geometry optimization, distance between O of carbonyl and Mg of MgO surface is 2.2 Å in both routes. (**Figure 21**) O-H distance of methylene route is 2.7 Å and 4.3 Å for methyl route. Since the methyl route has a larger distance, it affects to the force of deprotonation the proton to transform into an enolate form. O-H distance of methylene route is shorter than that of methyl route that leads to the stronger connections of atoms. From the transition state of enolization step, O-H distance of transition state of methylene route is 1.75 Å and 2.2 Å for methyl route (**Figure 22**). O-H distance of transition state methylene route is shorter than methyl route.

The transition state of C-C coupling step, C-C distance of transition state of methylene route is 2.2 Å and 1.6 Å for methyl route (**Figure 23**). C-C distance of transition state methylene route is larger than methyl route. Thus, enolization step of methylene route easier to connect than methyl route but the C-C coupling methyl route easier to react than methylene route that relate with the energy barrier in 4.3

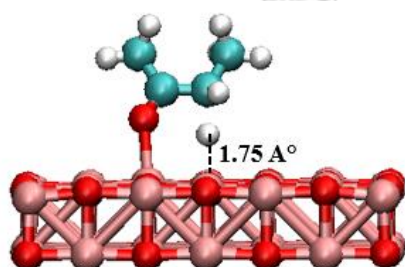
(a) Methylene route (S1)



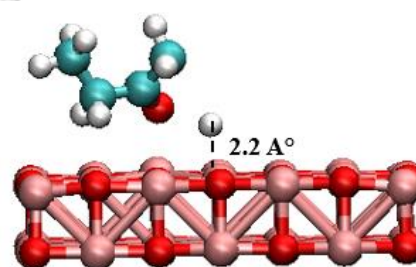
(b) Methyl route (S1)

**Figure 21** O-H distance of methylene route(a) and methyl route(b).

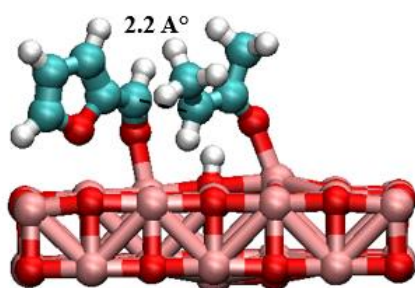
(a) Methylene route (S1)



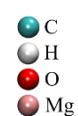
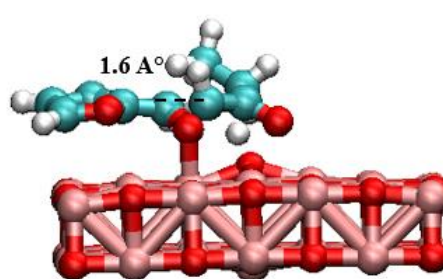
(b) Methyl route (S1)

**Figure 22** O-H distance of transition state of enolization step for methylene route(a) and methyl route(b).

(a) Methylene route (S1)



(b) Methyl route (S1)

**Figure 23** C-C distance of C-C coupling step for methylene route(a) and methyl route(b).

4.5 Thermodynamic properties

The calculation of thermodynamic properties was calculated to support and explain for more details. Thermodynamic property (Gibb free energy and enthalpy) of each step is shown in **Table 2**. The energy calculation (Gibb free energy and Enthalpy) of methylene route and methyl route are also reported in the same table. The methylene route energy and methyl route still follow the same pattern for three steps. The values are much stabilized in step 3 because product after dehydration is much stable. However, the values are not stabilized in step 1 because step 1 is the rate determining step.



Table 2 Thermodynamic property of each step (kcal/mol).

	Energy				
	S1	S2	S3	S4	S5
Methylene route					
ΔG	0	-0.62	46.62	4.39	-16.75
ΔH	0	-0.89	55.84	1.25	-18.01
Methyl route					
ΔG	0	-1.69	48.69	3.07	-17.32
(Linear product)					
ΔH	0	-4.39	59.36	0.87	-17.57

ΔG is relative Gibb free energy (kcal/mol).

ΔH is Enthalpy (kcal/mol).

Chapter 5 Conclusion and Recommendation

5.1 Conclusion

In summary, the aldol condensation between furfural and 2-butanone over MgO was investigated using DFT calculation. Three primary reaction steps were identified, including Step 1: Enolization of 2-butanone, Step 2: Addition of 2-butanone enolate, and Step 3: Internal dehydration to form the condensation product. The calculated energy profiles revealed that the energy barrier and the activation energy in enolization step obtained for the methylene route are lower than those obtained for the methyl route. The energy barrier and the activation energy in C-C coupling step obtained for methyl route are lower than those obtained for methylene route. The highest activation energy was found in the enolization step, evidence of the rate determining step. The reaction via methylene (branched product) is more favorable than the methyl product (linear product) as indicated by lower activation energy. Aldol condensation between furfural and 2-butanone over MgO, which is the base-catalyzed reaction. The steps of enolization and C-C coupling are easier to be occurred, however, it is difficult for dehydration step.

5.2 Recommendation

The effect of temperature and pressure on reaction mechanism should be considered since high temperatures and pressure affects the reaction activation energy. In addition, the dispersion force of system should be included in calculations for accurate prediction.

Appendices

The binding energy, E is defined using

$$E = E_{total} - E_{MgO} - E_{2-Butanone} \text{ -----(1)}$$

$$E = E_{total} - E_{MgO} - E_{2-Butanone} - E_{Furfural} \text{ -----(2)}$$

When E_{total} is energy of complex,

E_{MgO} , is energy of 2 layers MgO surface.

$E_{2-butanone}$ is energy of 2-butanone molecule.

and $E_{Furfural}$ is energy of furfural molecule.

Table 3 Binding energy of each step (kcal/mol).

	S 1	S 2	S 3	S 4	S 5
Methylene route (Branched product)	-11.28	1.56	-430605.44	-430636.64	-382702.36
Methyl route (Linear product)	-15.41	-8.98	-430591.31	-430633.94	-382458.36

Ex. Calculation of energy barrier of S2 for methylene route

$$E_{total} = -9870.969525 \text{ hartee}$$

$$E_{MgO} = -9638.687435 \text{ hartee}$$

$$E_{2-Butanone} = -232.2845817 \text{ hartee}$$

$$\text{From } E = E_{total} - E_{MgO} - E_{2-Butanone} \text{ -----(1)}$$

$$E = [(-9870.969525) - (-9638.687435) - (-232.2845817)] \times 627.5$$

$$= 1.56 \text{ kcal/mol } (\times 627.5 \text{ for convert unit from hartee to kcal/mol})$$

HOMO-LUMO

The global reactivity descriptors have been calculated by the help of Electronic density map of the highest occupied molecular orbital (HOMO) and lowest unoccupied molecular orbital (LUMO) energies to determine chemical stability, the HOMO-LUMO gap is where the most likely excitations can occur. The energy levels of molecular orbitals are computed by DFT-M062X/6-31G method and the diagrams of HOMO and LUMO are indicated in **Figure 24** and **Figure 25**. The HOMO-LUMO value of branched is 12.5496 kcal/mol and linear route is 12.5244 kcal/mol. From The HOMO-LUMO energy value were found that the energy values of both routes were only slightly different, so we could not tell the difference very much. This reaction was explained by using EA energy mainly for consider how different of product.

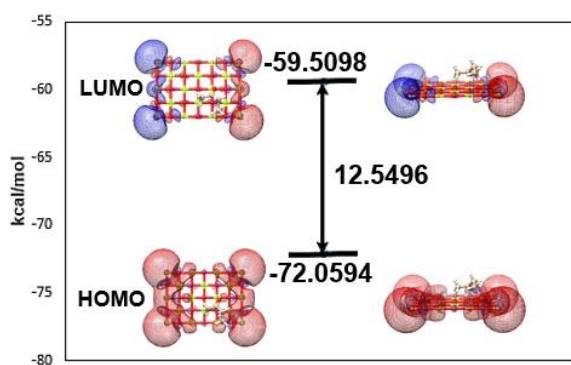


Figure 24 The DFT predicted HOMO-LUMO of 2-butanone on MgO (100) surface. (Methylene route).

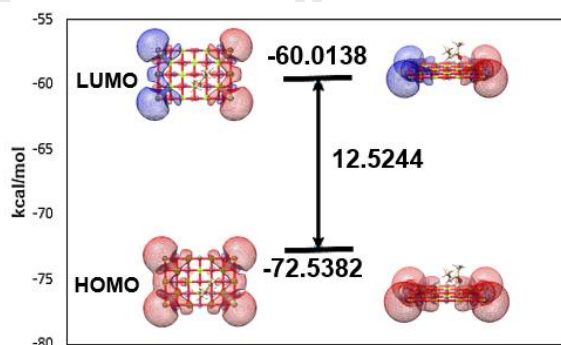


Figure 25 The DFT predicted HOMO-LUMO of 2-butanone on MgO (100) surface. (Methyl route).

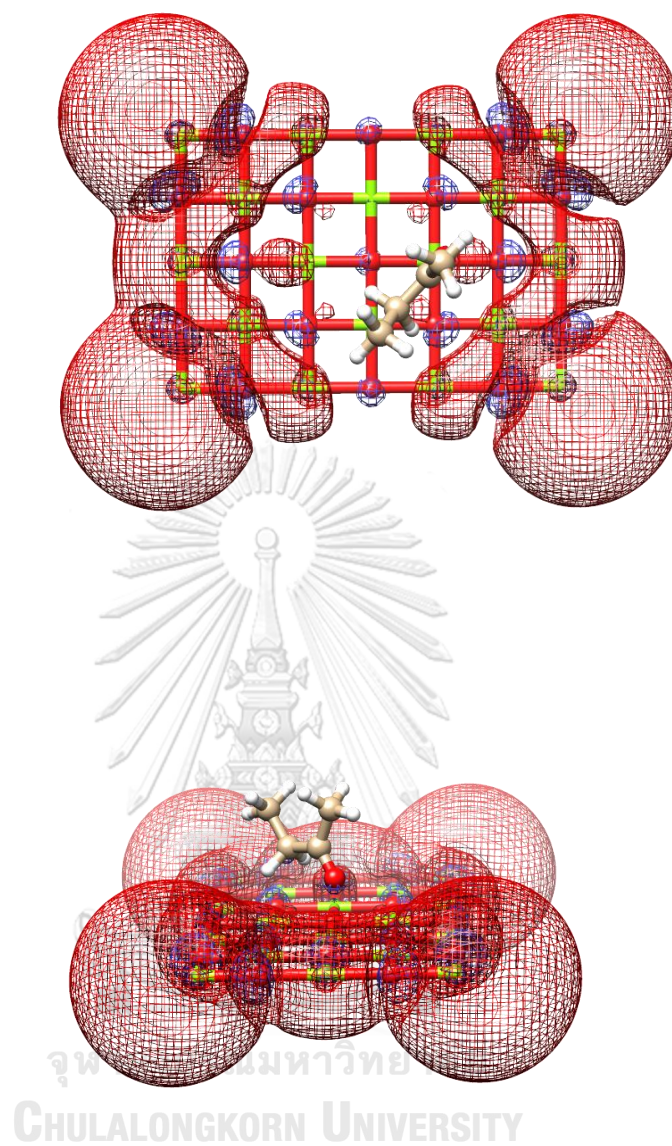


Figure 26 HOMO of 2-butanone on MgO (100) surface (1 layer). (Methylene route).

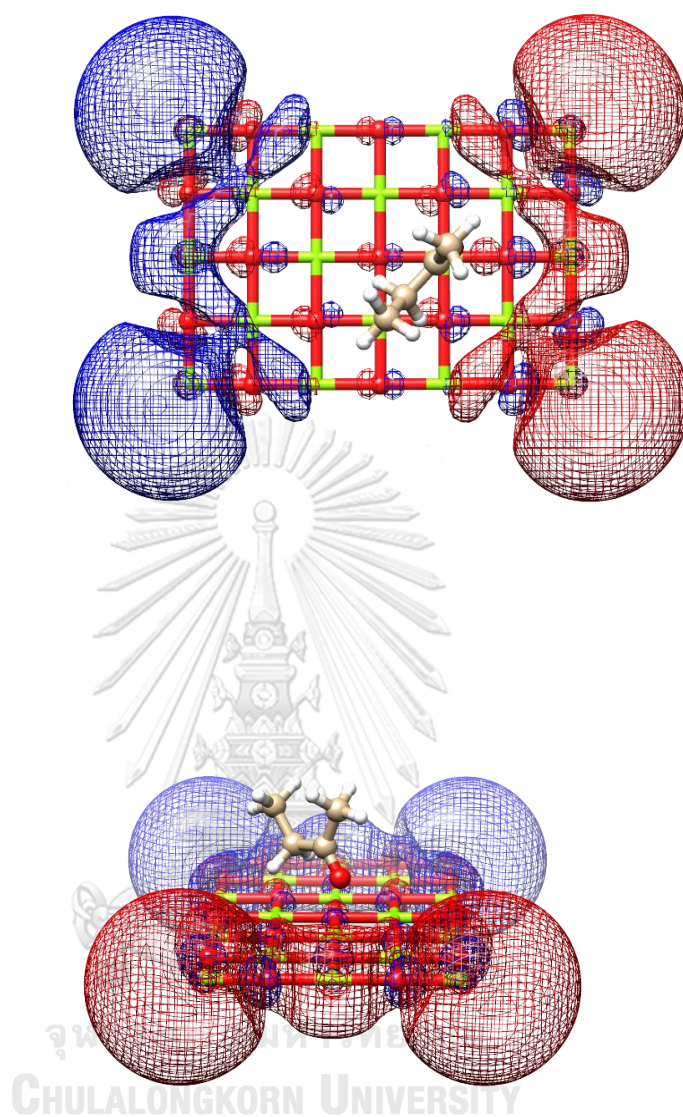


Figure 27 LUMO of 2-butanone on MgO (100) surface (1 layer). (Methylene route).

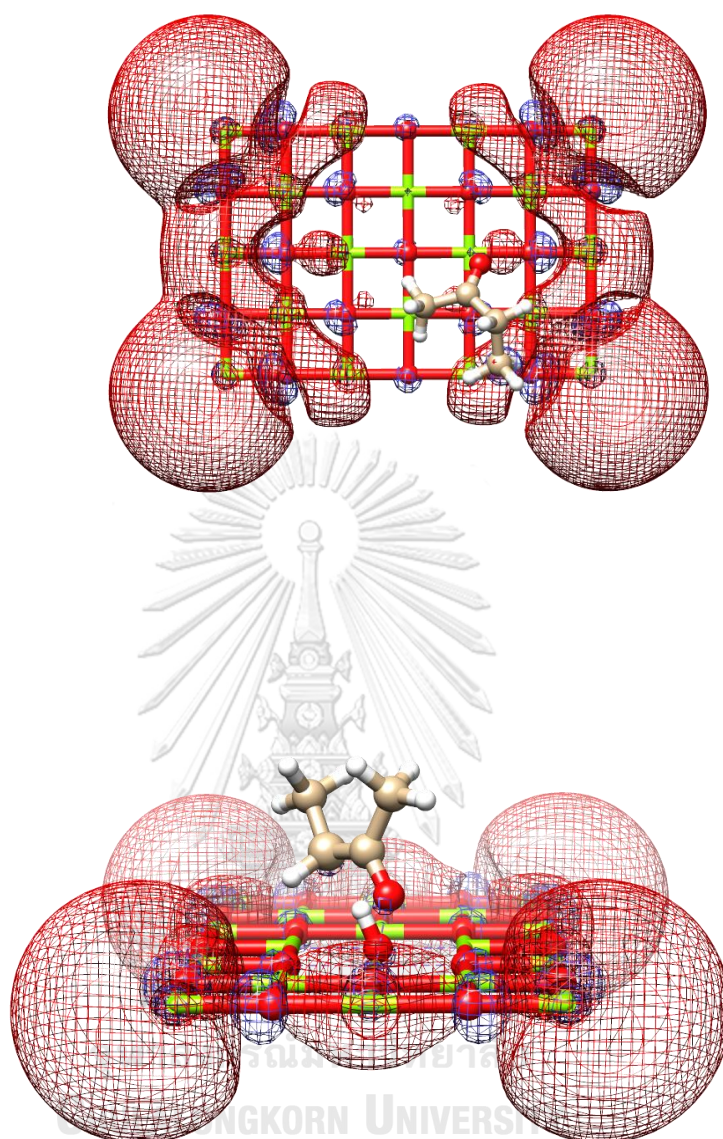


Figure 28 HOMO of 2-butanone on MgO (100) surface (1 layer). (Methyl route).

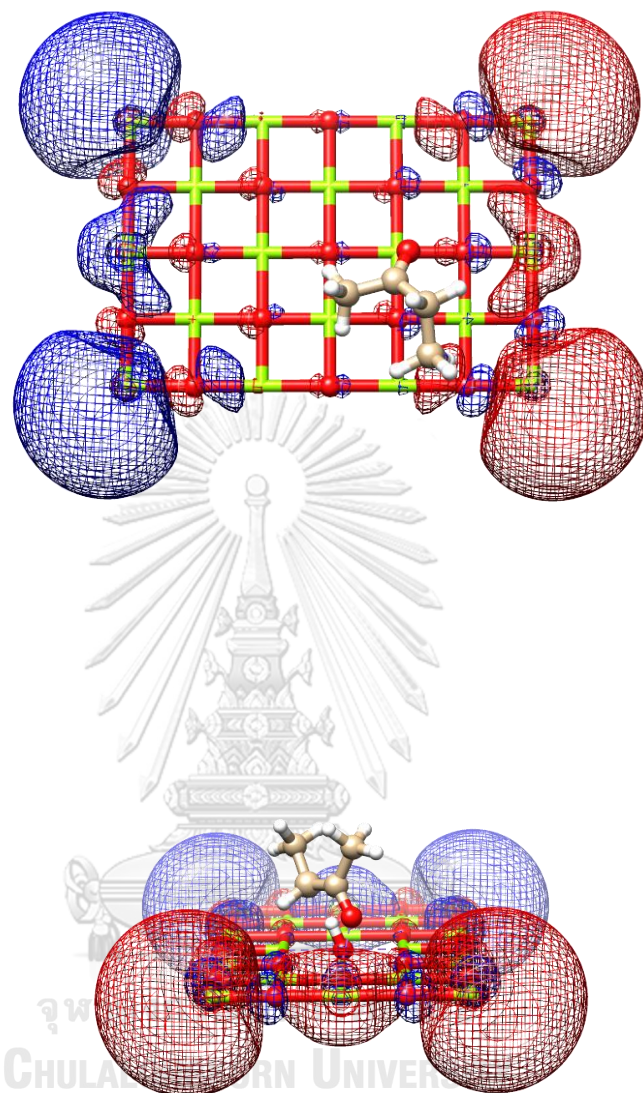


Figure 29 LUMO of 2-butanone on MgO (100) surface (1 layer). (Methyl route).

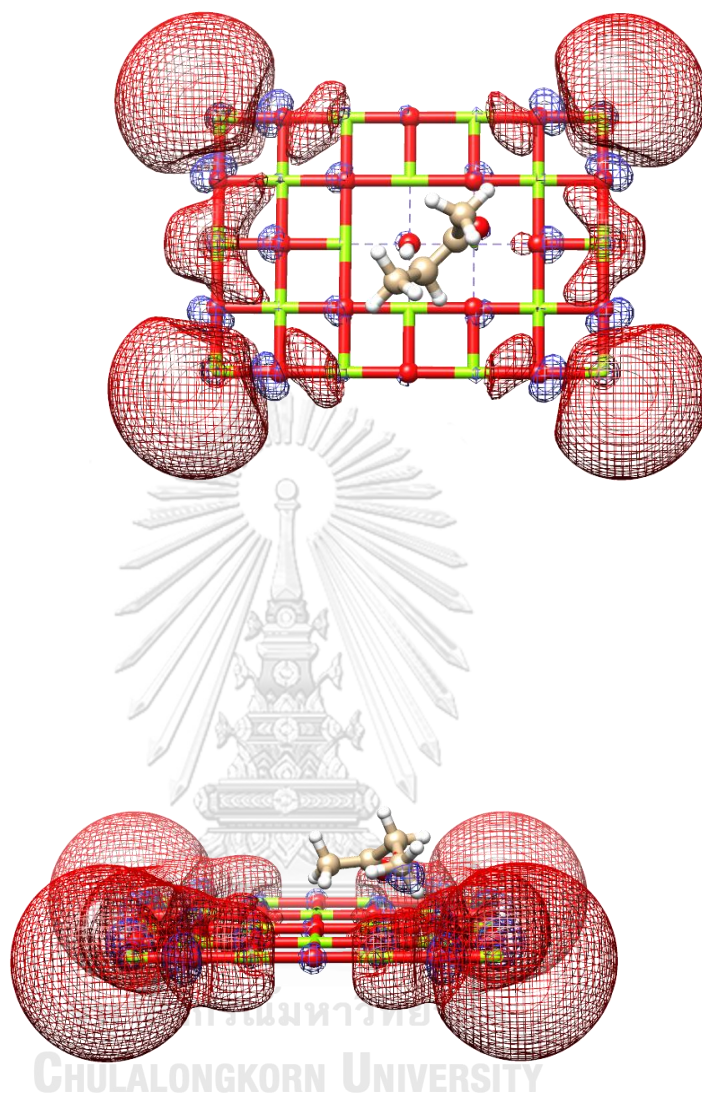


Figure 30 HOMO of 2-butanone enolate on MgO (100) surface (1 layer).
(Methylene route)

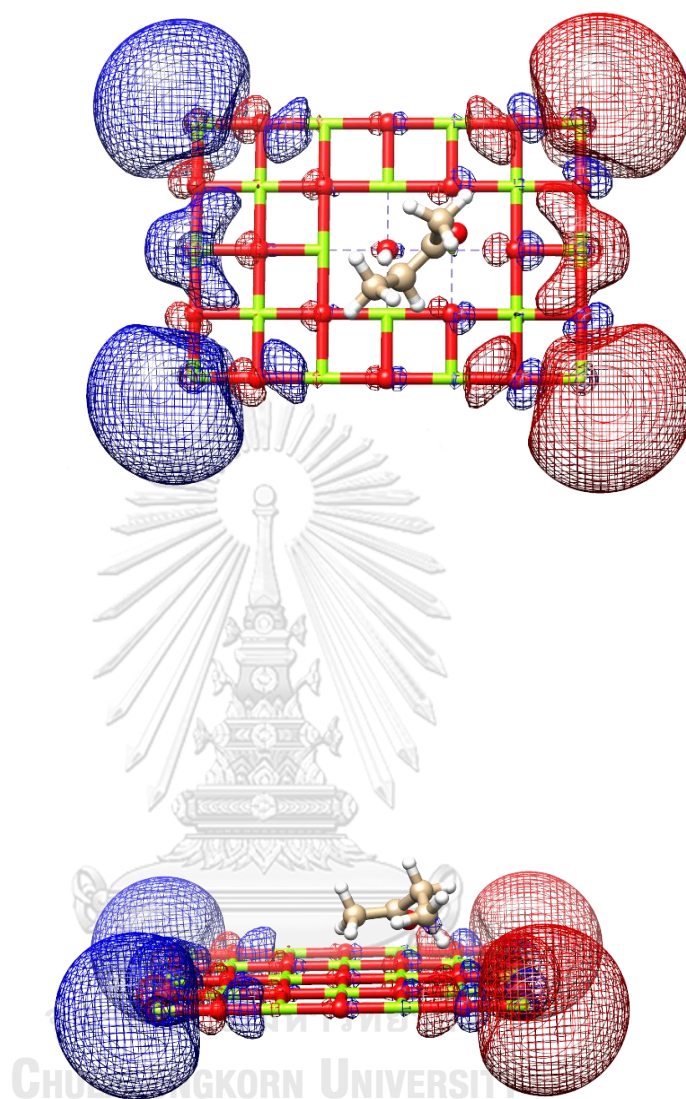


Figure 31 LUMO of 2-butanone enolate on MgO (100) surface (1 layer)
(Methylene route).

Code Input

- Optimization (S1: 2-butanone on MgO of methylene route)

```
%chk=B2L_1.chk
%mem=4GB
%nprocshared=16
# opt 6-31g geom=connectivity m062x

butanone2-MgO4

0 1
Mg
Mg          1      2.91656771
O           1      2.05368059      2      44.79599578
O           2      2.04297720      1      44.47955064      3
179.91362989  0
Mg          3      7.35235399      1     145.78815581      4 -
179.64632885  0
Mg          5      2.89387882      3     100.97176695      1
179.95351124  0
O           5      2.03691042      3     145.84748374      1
179.92839086  0
Mg          1      4.06098171      4     179.55423647      2 -
22.12262344   0
Mg          3      2.04259692      1      89.52523413      4 -
179.98887835  0
O           9      2.04108637      3     179.55170318      1
131.93306867  0
Mg         10      2.03665677      9      90.54076875      3
48.06532855   0
O           5      2.03319600      3      34.04300174      1
-0.08701395   0
Mg          6      2.89377320      5      90.30750700      3
0.04297829    0
Mg         13      2.88658600      6      90.25894159      5 -
179.85799395  0
O         13      2.03736426      6      44.85353347      5 -
179.94186988  0
Mg          3      2.03764605      1     179.88716251      4
89.25148293   0
Mg         13      2.90181323      6     179.51592916      5 -
161.58821761  0
O         13      2.03188443      6     135.04916004      5
0.09839423    0
O           2      2.03351355      1     135.84251914      4 -
179.93222011  0
O         14      2.03256653     13      46.01580531      6
179.89366456  0
O           1      2.03034158      4     179.69010826      2 -
152.85890681  0
```

Mg		18	2.05812189	13	89.82489444	6
-0.09234365	0					
O		22	2.03411013	18	89.93373768	13
179.90074057	0					
O		22	2.03511917	18	89.97523134	13
0.02456168	0					
Mg		15	2.05441581	13	179.93721637	6
141.21066417	0					
O		14	2.04053597	13	134.36777002	6
-0.07094420	0					
Mg		7	2.05435193	5	179.89611956	3 -
141.64792007	0					
O		25	2.03333354	15	90.83349432	13 -
141.24481650	0					
Mg		4	1.98985436	2	88.49363607	1
88.45367464	0					
Mg		3	2.06924464	1	89.90251189	21 -
90.14751168	0					
O		29	1.99105556	4	93.30543093	2
1.85289771	0					
O		29	1.99037595	4	93.31389177	2 -
92.93408224	0					
Mg		7	2.06871849	5	90.22044500	3
90.17053621	0					
Mg		10	2.07426349	9	89.97063666	3
138.11679859	0					
Mg		32	2.03916294	29	176.55520222	4
54.38577632	0					
O		35	2.03766219	32	178.92364430	29 -
155.05715400	0					
Mg		23	2.12456509	22	90.06969297	18 -
89.53835868	0					
Mg		12	2.07040840	5	90.04773925	3 -
90.28874614	0					
O		38	2.02841301	12	90.87163335	5
179.73214732	0					
O		38	2.03806948	12	90.54591480	5
0.12479437	0					
Mg		15	2.07156944	13	90.20181635	6 -
90.22961774	0					
Mg		31	2.03606718	29	176.64049742	4 -
52.83688572	0					
Mg		20	2.04956606	14	89.96008305	13
89.39139428	0					
O		43	2.03167772	20	90.38612948	14
0.80726157	0					
Mg		18	2.10775088	13	90.36001853	6
90.53259682	0					
O		43	2.03760077	20	90.66202379	14
179.92776287	0					
O		45	2.02738448	18	89.64193851	13 -
179.98213016	0					

O		41	2.04366336	15	90.63518616	13
-0.14903780	0					
Mg		40	2.05844372	38	90.37522426	12
89.60755353	0					
O		49	2.04054559	40	90.04887988	38 -
179.52739443	0					
O		35	2.02610164	32	90.48841782	29
38.27736303	0					
O		49	2.03281000	40	89.98088182	38
0.36186271	0					
Mg		26	1.99014672	14	88.70057117	13 -
88.31686103	0					
O		53	1.99548392	26	93.68658668	14
92.56808520	0					
Mg		54	2.03191672	53	176.50979789	26 -
43.94367862	0					
O		55	2.03072863	54	178.88553006	53
179.63668087	0					
Mg		10	2.05438257	9	179.89279320	3 -
125.11508815	0					
O		8	2.04201150	1	179.55453235	21
154.06898400	0					
Mg		7	2.05622131	5	89.66956424	3 -
179.93570382	0					
Mg		12	2.06538192	5	90.20143069	3
179.94835914	0					
O		57	2.03172734	10	91.08297375	9
173.07696903	0					
O		59	2.03281356	7	90.90834464	5
-0.01491614	0					
O		59	2.04101905	7	89.46531385	5
179.96603470	0					
Mg		36	1.99165272	35	176.53187165	32
153.13275154	0					
O		64	1.99103546	36	94.56600142	35
41.10638371	0					
Mg		39	2.03474834	38	90.01114119	12
88.94067048	0					
Mg		40	2.04806079	38	89.73792304	12 -
89.01128771	0					
O		67	2.03088634	40	90.04614624	38
179.77071877	0					
O		67	2.03414190	40	90.80242191	38
-1.32734838	0					
Mg		63	1.99217162	59	88.67073596	7
88.29263173	0					
C		49	3.80221652	40	99.43225188	38
76.95431376	0					
C		71	1.57798524	49	51.04188332	40 -
91.90243531	0					
C		72	1.52370688	71	120.22873698	49
165.25191549	0					

C		73	1.53533662	72	122.15029173	71
13.56750140	0					
O		73	1.32181267	72	116.50682865	71 -
177.76404726	0					
H		71	1.09703269	49	165.94749480	40 -
97.33871170	0					
H		71	1.09761282	49	81.74726250	40
33.27066756	0					
H		71	1.09833520	49	80.31183511	40
142.62213989	0					
H		72	1.09477168	71	106.27915810	49
56.39400213	0					
H		72	1.11260695	71	108.25432989	49 -
62.58528614	0					
H		74	1.09024311	73	107.20383495	72
164.91140666	0					
H		74	1.10201784	73	110.08683138	72
44.96337827	0					
H		74	1.10248582	73	112.93684631	72 -
74.64612894	0					

1 3 1.0 4 1.0 21 1.0 29 1.0 32 1.0
 2 3 1.0 4 1.0 16 1.0 19 1.0 29 1.0 31 1.0
 3 9 1.0 16 1.0 30 1.0
 4 29 1.0
 5 7 1.0 12 1.0 24 1.0 40 1.0 62 1.0
 6 7 1.0 15 1.0 24 1.0 28 1.0 50 1.0
 7 27 1.0 33 1.0 59 1.0
 8 10 1.0 21 1.0 36 1.0 58 1.0 64 1.0
 9 10 1.0 21 1.0 23 1.0 51 1.0
 10 11 1.0 34 1.0 57 1.0
 11 12 1.0 23 1.0 39 1.0 57 1.0 61 1.0
 12 22 1.0 38 1.0 60 1.0
 13 15 1.0 18 1.0 20 1.0 24 1.0 48 1.0
 14 15 1.0 20 1.0 26 1.0 44 1.0 53 1.0
 15 25 1.0 41 1.0
 16 18 1.0 19 1.0 23 1.0 47 1.0
 17 18 1.0 19 1.0 20 1.0 46 1.0
 18 22 1.0 45 1.0
 19 42 1.0
 20 43 1.0
 21 35 1.0
 22 23 1.0 24 1.0 52 1.0
 23 37 1.0
 24 49 1.0
 25 26 1.0 28 1.0 53 1.0 54 1.0
 26 53 1.0
 27 28 1.0 56 1.0 63 1.0 70 1.0
 28 55 1.0
 29 30 1.0 31 1.0 32 1.0
 30 31 1.0 32 1.0 47 1.0 51 1.0
 31 42 1.0
 32 35 1.0

33 40 1.0 50 1.0 56 1.0 68 1.0 70 1.0
 34 36 1.0 39 1.0 51 1.0 64 1.0 65 1.0
 35 36 1.0 51 1.0
 36 64 1.0
 37 39 1.0 47 1.0 51 1.0 52 1.0 75 0.5
 38 39 1.0 40 1.0 52 1.0 66 1.0 67 1.0 69 1.0
 39 66 1.0
 40 49 1.0 67 1.0
 41 44 1.0 48 1.0 50 1.0 53 1.0 54 1.0
 42 45 1.0 46 1.0 47 1.0
 43 44 1.0 46 1.0 48 1.0
 44 53 1.0
 45 46 1.0 47 1.0 48 1.0 52 1.0
 46
 47
 48 49 1.0
 49 50 1.0 52 1.0
 50 55 1.0
 51
 52
 53 54 1.0
 54 55 1.0
 55 56 1.0
 56 70 1.0
 57 58 1.0 61 1.0 64 1.0 65 1.0
 58 64 1.0
 59 62 1.0 63 1.0 68 1.0 70 1.0
 60 61 1.0 62 1.0 69 1.0
 61 66 1.0
 62 67 1.0
 63 70 1.0
 64 65 1.0
 65 66 1.0
 66 69 1.0
 67 68 1.0 69 1.0
 68 70 1.0
 69
 70
 71 72 1.0 76 1.0 77 1.0 78 1.0
 72 73 1.0 79 1.0 80 1.0
 73 74 1.0 75 2.0
 74 81 1.0 82 1.0 83 1.0
 75
 76
 77
 78
 79
 80
 81
 82
 83



จุฬาลงกรณ์มหาวิทยาลัย
 CHULALONGKORN UNIVERSITY

- Optimization (S1: 2-butanone on MgO of methyl route)

```
%chk=S2L_1.chk
%mem=4GB
%nprocshared=12
# opt 6-31g geom=connectivity m062x
```

butanone2-MgO4

```
0 1
Mg      0.00000000    0.00000000    0.00000000
Mg      0.00000000    0.00000000    2.91656771
O       1.44699176    0.00000000    1.45733278
O      -1.43141986    0.00215779    1.45890232
Mg      8.66441579    0.02115261    2.85927861
Mg      8.66339654    0.01302075    5.75314583
O     10.10108243    0.02259257    4.30322838
Mg      2.86493709    0.00757938   -2.87813315
Mg     -2.88448378   -0.00176009    0.00618987
O      4.32845789    0.00836146   -1.43633220
Mg      5.78140161    0.00847739   -0.00912328
O      7.22761775    0.01939338    1.42070491
Mg      5.76968557    0.00074984    5.76762305
Mg      5.77108533   -0.00019701    8.65420855
O      7.22116634    0.00432703    7.19732368
Mg      2.88264283   -0.00401251    2.90332424
Mg      2.86812223   -0.00387640    5.80542244
O      4.32453667   -0.00381185    4.33930999
O      1.41661235   -0.00045963    4.37546681
O      4.30790973   -0.00321930    7.24338087
O      1.41496370    0.00287652   -1.45607568
Mg      5.77572543    0.00724368    2.87992838
O      4.33173346   -0.00082611    1.44729930
O      7.21818031    0.01090211    4.31555387
Mg      8.68355699    0.00933696    8.64024183
O      7.23048058    0.00371227   10.08037028
Mg     11.55211123    0.02636788    5.75748525
O     10.13255341    0.01683654    7.21377822
Mg     -1.35946737   -1.98639524    1.45861523
Mg      1.44281131   -2.06924026    1.45652204
O     -0.01057547   -2.05267576    2.92162576
O     -0.01103455   -2.05252442   -0.00390051
Mg     10.11807965   -2.04605293    4.29960771
Mg      4.33368075   -2.06588071   -1.44415400
Mg      1.44143499   -2.04622487   -1.43515103
O      2.86634118   -2.04804155   -2.89175882
Mg      4.33185714   -2.12537547    1.45547265
Mg      7.24069918   -2.05093305    1.40773329
O      5.80093819   -2.08193805   -0.02075763
O      8.67786575   -2.07032487    2.85269122
Mg      7.22930487   -2.06721350    7.20464241
Mg      1.43658818   -2.04578735    4.35384065
```

Mg	4.32893244	-2.05262002	7.22802554
O	5.77155016	-2.06223316	8.65857651
Mg	4.31027086	-2.11151317	4.34163487
O	2.86070478	-2.08064211	5.81546078
O	2.86893870	-2.09066011	2.91600709
O	5.76980887	-2.10065624	5.77449804
Mg	7.22790869	-2.07467061	4.31378540
O	8.67507782	-2.07723070	5.75236847
O	2.87559821	-2.08511701	-0.00450393
O	5.78548181	-2.06819340	2.88141700
Mg	7.24501442	-1.98500529	10.00637573
O	8.69940458	-2.05200155	8.64174507
Mg	10.12245725	-2.02919931	7.19154276
O	11.56386627	-2.03529459	5.76110170
Mg	5.77913677	0.01900533	-2.89094735
O	4.31540803	0.01886161	-4.31542844
Mg	11.55030855	0.03328616	2.84457305
Mg	8.68380213	0.02921775	-0.04395649
O	7.24457310	0.02291156	-1.48368153
O	10.13114117	0.03142675	1.38913790
O	12.98470087	0.03590101	4.29656155
Mg	4.32340632	-1.97382671	-4.24753678
O	5.79243070	-2.03900267	-2.90517258
Mg	7.23263522	-2.02623066	-1.46552096
Mg	10.12321467	-2.01667826	1.40264242
O	11.56293290	-2.02759174	2.83498025
O	8.70342565	-2.04392522	-0.05378815
Mg	12.91918303	-1.95519014	4.29990896
C	6.71223383	-7.52056476	4.15791593
C	7.08846518	-6.04714044	4.57923304
C	6.68277687	-4.87061255	3.70009607
C	5.65760799	-5.01334595	2.56611437
O	7.07502535	-3.67310443	4.09922534
H	5.93561397	-7.59757122	3.38693452
H	7.59536913	-8.05397461	3.78334967
H	6.33990463	-8.07384021	5.03061145
H	8.17085903	-5.95584969	4.44279773
H	6.81341797	-5.90941167	5.64847298
H	5.34828950	-4.00710704	2.28250307
H	4.78886504	-5.59626561	2.91242879
H	6.06396578	-5.53227874	1.68234003

1 3 1.0 4 1.0 21 1.0 29 1.0 32 1.0
2 3 1.0 4 1.0 16 1.0 19 1.0 29 1.0 31 1.0
3 9 1.0 16 1.0 30 1.0
4 29 1.0
5 7 1.0 12 1.0 24 1.0 40 1.0 62 1.0
6 7 1.0 15 1.0 24 1.0 28 1.0 50 1.0
7 27 1.0 33 1.0 59 1.0
8 10 1.0 21 1.0 36 1.0 58 1.0 64 1.0
9 10 1.0 21 1.0 23 1.0 51 1.0
10 11 1.0 34 1.0 57 1.0
11 12 1.0 23 1.0 39 1.0 57 1.0 61 1.0

12 22 1.0 38 1.0 60 1.0
 13 15 1.0 18 1.0 20 1.0 24 1.0 48 1.0
 14 15 1.0 20 1.0 26 1.0 44 1.0 53 1.0
 15 25 1.0 41 1.0
 16 18 1.0 19 1.0 23 1.0 47 1.0
 17 18 1.0 19 1.0 20 1.0 46 1.0
 18 22 1.0 45 1.0
 19 42 1.0
 20 43 1.0
 21 35 1.0
 22 23 1.0 24 1.0 52 1.0
 23 37 1.0
 24 49 1.0
 25 26 1.0 28 1.0 53 1.0 54 1.0
 26 53 1.0
 27 28 1.0 56 1.0 63 1.0 70 1.0
 28 55 1.0
 29 30 1.0 31 1.0 32 1.0
 30 31 1.0 32 1.0 47 1.0 51 1.0
 31 42 1.0
 32 35 1.0
 33 40 1.0 50 1.0 56 1.0 68 1.0 70 1.0
 34 36 1.0 39 1.0 51 1.0 64 1.0 65 1.0
 35 36 1.0 51 1.0
 36 64 1.0
 37 39 1.0 47 1.0 51 1.0 52 1.0
 38 39 1.0 40 1.0 52 1.0 66 1.0 67 1.0 69 1.0
 39 66 1.0
 40 49 1.0 67 1.0
 41 44 1.0 48 1.0 50 1.0 53 1.0 54 1.0
 42 45 1.0 46 1.0 47 1.0
 43 44 1.0 46 1.0 48 1.0
 44 53 1.0
 45 46 1.0 47 1.0 48 1.0 52 1.0
 46
 47
 48 49 1.0
 49 50 1.0 52 1.0 75 0.5
 50 55 1.0
 51
 52 81 0.5
 53 54 1.0
 54 55 1.0
 55 56 1.0
 56 70 1.0
 57 58 1.0 61 1.0 64 1.0 65 1.0
 58 64 1.0
 59 62 1.0 63 1.0 68 1.0 70 1.0
 60 61 1.0 62 1.0 69 1.0
 61 66 1.0
 62 67 1.0
 63 70 1.0
 64 65 1.0

65 66 1.0
66 69 1.0
67 68 1.0 69 1.0
68 70 1.0
69
70
71 72 1.0 76 1.0 77 1.0 78 1.0
72 73 1.0 79 1.0 80 1.0
73 74 1.0 75 2.0
74 81 1.0 82 1.0 83 1.0
75
76
77
78
79
80
81
82
83



จุฬาลงกรณ์มหาวิทยาลัย
CHULALONGKORN UNIVERSITY

- For TS

```
%chk=TS_B12.chk
%mem=8GB
%nprocshared=12
# opt=ts 6-31g geom=connectivity m062x modredundant
```

Molecule Name

```
0 1
Mg      0.00000000    0.00000000    0.00000000
Mg      0.00000000    0.00000000    2.83991438
O       1.41361941    0.00000000    1.42048263
O      -1.37986038    0.09464504    1.41856897
Mg      8.46375757   -0.38041081    2.78560067
Mg      8.46496600   -0.39435066    5.63690585
O       9.85547564   -0.42541549    4.21062977
Mg      2.80040100   -0.13417694   -2.81327309
Mg      2.80935807   -0.11666075   -0.00002506
O       4.22679763   -0.14488794   -1.40511796
Mg      5.64102265   -0.26581081   -0.01269031
O       7.06293033   -0.28257138    1.38316231
Mg      5.61718655   -0.25311675    5.65550957
Mg      5.63306844   -0.31520592    8.46152764
O       7.04910852   -0.31126548    7.03758997
Mg      2.80418406   -0.10502315    2.84176970
Mg      2.78539609   -0.17196391    5.68059984
O       4.21190000   -0.12956517    4.25946340
O       1.34028375   -0.00264284    4.31700149
O       4.16794271   -0.17587247    7.12596348
O       1.34765773   -0.00666662   -1.46305219
Mg      5.62328841   -0.27659038    2.81144600
O       4.22948228   -0.15188194    1.41100532
O       7.04638194   -0.27714604    4.22439056
Mg      8.46947348   -0.44766310    8.44633734
O       7.06021324   -0.36628590    9.83424261
Mg     11.27078836   -0.55459658    5.62529969
O       9.92592005   -0.44800540    7.08922387
Mg     -1.35834854   -1.81285696    1.41904235
Mg      1.30944329   -2.13552388    1.41524913
O      -0.14327367   -2.08530329    2.89937118
O      -0.14024823   -2.08860992   -0.05860252
Mg      9.77988259   -2.55394200    4.19428481
Mg      4.12794560   -2.27954095   -1.42247564
Mg      1.29912240   -2.04747008   -1.42259964
O       2.64609524   -2.22257850   -2.86309993
Mg      4.10921997   -2.40940349    1.40600622
Mg      6.97027113   -2.40868273    1.36500539
O       5.55779261   -2.40666407   -0.03229528
O       8.37416643   -2.53024875    2.77838569
Mg      6.95272375   -2.43946422    7.03560874
Mg      1.29035224   -2.03717532    4.26702874
```

Mg	4.11045959	-2.21192892	7.06264940
O	5.48002359	-2.40191586	8.48319072
Mg	4.09653459	-2.25203507	4.24156722
O	2.64442869	-2.21752008	5.71892310
O	2.68624370	-2.20711565	2.85520404
O	5.51818950	-2.40931305	5.63928570
Mg	6.95381513	-2.39736629	4.21001470
O	8.36829894	-2.54040591	5.62301011
O	2.70209157	-2.22958237	-0.01878028
O	5.54145109	-2.38882781	2.81891877
Mg	6.97005921	-2.26853148	9.71245186
O	8.43158725	-2.54027124	8.47008623
Mg	9.79466549	-2.48290475	7.03176517
O	11.21670905	-2.64986434	5.67007023
Mg	5.63235626	-0.26935352	-2.82142533
O	4.21384254	-0.17018142	-4.20263864
Mg	11.26617540	-0.54036282	2.78747831
Mg	8.46865151	-0.43021508	-0.04437218
O	7.10363566	-0.28752138	-1.48241418
O	9.92340590	-0.41696125	1.32692845
O	12.64964193	-0.58672953	4.20717194
Mg	4.12730656	-2.07415893	-4.09968879
O	5.60020068	-2.35813683	-2.87586391
Mg	6.97996658	-2.32401075	-1.45163421
Mg	9.79228408	-2.45247782	1.34790636
O	11.21674953	-2.63040145	2.71661867
O	8.43783495	-2.47776021	-0.10277045
Mg	12.45962159	-2.48647311	4.19262818
C	4.54854182	-6.72956293	4.52608838
C	4.65464874	-5.57901079	3.52748947
C	3.63146794	-5.53831175	2.40219431
C	2.65584459	-6.67473865	2.22530340
O	3.54061769	-4.56247277	1.68052803
H	3.59402620	-6.70270924	5.05931280
H	4.64546552	-7.70911110	4.05362275
H	5.34027533	-6.64337019	5.27326867
H	5.64447182	-5.54090865	3.05702955
H	5.36557637	-4.12788657	2.90402294
H	2.06750923	-6.50550829	1.32441370
H	1.98409948	-6.69230163	3.09195136
H	3.15304288	-7.64502202	2.18488180

1 2 1.0 3 1.0 4 1.0 9 1.0 21 1.0 29 1.0 30 1.0 32 1.0 35 1.0
2 3 1.0 4 1.0 16 1.0 19 1.0 29 1.0 30 1.0 31 1.0 42 1.0
3 9 1.0 16 1.0 30 1.0
4 29 1.0
5 6 1.0 7 1.0 12 1.0 22 1.0 24 1.0 59 1.0 60 1.0 62 1.0 67
1.0
6 7 1.0 13 1.0 15 1.0 24 1.0 25 1.0 27 1.0 28 1.0 55 1.0
7 27 1.0 33 1.0 59 1.0
8 9 1.0 10 1.0 21 1.0 34 1.0 35 1.0 36 1.0 57 1.0 58 1.0 64
1.0
9 10 1.0 11 1.0 16 1.0 21 1.0 23 1.0 35 1.0 51 1.0

10 11 1.0 34 1.0 57 1.0
 11 12 1.0 22 1.0 23 1.0 38 1.0 57 1.0 60 1.0 61 1.0 66 1.0
 12 22 1.0 38 1.0 60 1.0
 13 14 1.0 15 1.0 17 1.0 18 1.0 20 1.0 22 1.0 24 1.0 43 1.0 45
 1.0
 14 15 1.0 20 1.0 25 1.0 26 1.0 41 1.0 43 1.0 44 1.0 53 1.0
 15 25 1.0 41 1.0
 16 17 1.0 18 1.0 19 1.0 22 1.0 23 1.0 42 1.0 45 1.0 47 1.0
 17 18 1.0 19 1.0 20 1.0 42 1.0 43 1.0 45 1.0 46 1.0
 18 22 1.0 45 1.0
 19 42 1.0
 20 43 1.0
 21 35 1.0
 22 23 1.0 24 1.0 45 1.0 49 1.0 52 1.0
 23
 24 49 1.0
 25 26 1.0 28 1.0 41 1.0 53 1.0 54 1.0 55 1.0
 26 53 1.0
 27 28 1.0 33 1.0 55 1.0 56 1.0 59 1.0 63 1.0 70 1.0
 28 55 1.0
 29 30 1.0 31 1.0 32 1.0
 30 31 1.0 32 1.0 35 1.0 37 1.0 42 1.0 47 1.0 51 1.0
 31 42 1.0
 32 35 1.0
 33 40 1.0 49 1.0 50 1.0 55 1.0 56 1.0 59 1.0 67 1.0 68 1.0 70
 1.0
 34 35 1.0 36 1.0 37 1.0 39 1.0 51 1.0 57 1.0 64 1.0 65 1.0 66
 1.0
 35 36 1.0 51 1.0
 36 64 1.0
 37 38 1.0 39 1.0 45 1.0 47 1.0 51 1.0 52 1.0 75 1.0
 38 39 1.0 40 1.0 49 1.0 52 1.0 60 1.0 66 1.0 67 1.0 69 1.0
 39 66 1.0
 40 49 1.0 67 1.0
 41 43 1.0 44 1.0 48 1.0 49 1.0 50 1.0 53 1.0 54 1.0 55 1.0
 42 45 1.0 46 1.0 47 1.0
 43 44 1.0 45 1.0 46 1.0 48 1.0
 44 53 1.0
 45 46 1.0 47 1.0 48 1.0 49 1.0 52 1.0
 46
 47
 48 49 1.0
 49 50 1.0 52 1.0
 50 55 1.0
 51
 52
 53 54 1.0
 54 55 1.0
 55 56 1.0
 56 70 1.0
 57 58 1.0 61 1.0 64 1.0 65 1.0 66 1.0
 58 64 1.0
 59 62 1.0 63 1.0 67 1.0 68 1.0 70 1.0

60 61 1.0 62 1.0 66 1.0 67 1.0 69 1.0
61 66 1.0
62 67 1.0
63 70 1.0
64 65 1.0
65 66 1.0
66 69 1.0
67 68 1.0 69 1.0
68 70 1.0
69
70
71 72 1.0 76 1.0 77 1.0 78 1.0
72 73 1.0 79 1.0
73 74 1.0 75 1.0
74 81 1.0 82 1.0 83 1.0
75
76
77
78
79
80
81
82
83



- Single point

```
%chk=EB1.chk
%mem=4GB
%nprocshared=12
# freq 6-31g geom=connectivity m062x
```

Title Card Required

```
0 1
Mg -1 5.89338900 -2.09258900 -1.30510400
Mg -1 3.88780500 -4.10010500 -1.19290100
O -1 3.88958700 -2.10198000 -1.33616900
O -1 5.86972200 -4.07307500 -1.25833900
Mg -1 -2.07069000 1.92139800 -1.33769600
Mg -1 -4.08539400 -0.09234900 -1.21115400
O -1 -4.06292100 1.89662800 -1.32227300
Mg -1 5.89580700 1.87634000 -1.45523800
Mg -1 3.90301000 -0.10725800 -1.36210900
O -1 3.89157000 1.88544400 -1.47686100
Mg -1 1.90527700 1.90501800 -1.38844600
O -1 -0.08728400 1.92004800 -1.40426500
Mg -1 -2.08060200 -2.11953300 -1.17564000
Mg -1 -4.07449100 -4.08748700 -1.00375900
O -1 -4.07116600 -2.08473900 -1.15135400
Mg -1 1.89995500 -2.12062600 -1.26105300
Mg -1 -0.09267400 -4.13578800 -1.08087400
O -1 -0.09812400 -2.13042400 -1.26735700
O -1 1.89588400 -4.20092300 -1.21456700
O -1 -2.09201200 -4.18433900 -1.10517200
O -1 5.97253600 -0.10952600 -1.43947100
Mg -1 -0.07684600 -0.10315300 -1.26500500
O -1 1.90075700 -0.10286500 -1.35872600
O -1 -2.08197800 -0.10042000 -1.29637700
Mg -1 -6.07352500 -2.07126400 -1.04721100
O -1 -6.05491500 -4.04991600 -0.98661200
Mg -1 -6.06577000 1.90181000 -1.22483400
O -1 -6.14605100 -0.08707800 -1.19033500
Mg -1 5.82404100 -3.92181300 0.64267500
Mg 0 3.92211600 -2.01200700 0.84021900
O -1 3.91428500 -4.09379600 0.89797400
O -1 6.00101000 -2.00038700 0.78420700
Mg 0 -4.02114300 1.99430500 0.83575900
Mg 0 3.93080400 1.96460800 0.67736600
Mg -1 5.94615700 -0.02633600 0.60047300
O -1 6.00719500 1.95232900 0.63508200
Mg 0 1.95361500 -0.02389200 0.92456100
Mg 0 -0.04349400 2.00414700 0.72410600
O 0 1.94173300 2.01419500 0.72180400
O 0 -2.03353000 2.01129500 0.78898100
Mg 0 -4.02514900 -1.99486700 1.00749700
Mg -1 1.93436600 -4.05518700 0.81562900
```

Mg	-1	-2.03876500	-4.03439300	0.92646800
O	-1	-4.01442200	-4.06121500	1.08764300
Mg	0	-0.04038600	-2.04145200	0.89863000
O	-1	-0.05218500	-4.11573800	0.96935300
O	0	1.93724500	-2.05720800	0.83858300
O	0	-2.03812300	-2.02608400	0.94620700
Mg	0	-2.04126900	-0.01627200	0.82707300
O	0	-4.04049000	-0.00039500	0.91181600
O	0	3.95863500	-0.02369100	0.72618700
O	0	-0.06020400	-0.01619000	0.84157000
Mg	-1	-5.93510100	-3.89113800	0.91131200
O	-1	-6.09647900	-1.96500200	1.04305000
Mg	-1	-6.04462600	0.00679000	0.84492600
O	-1	-6.09221300	1.98194200	0.86987600
Mg	-1	3.89489200	3.88455500	-1.49535700
O	-1	5.87590800	3.85573300	-1.56138500
Mg	-1	-4.05818700	3.90353000	-1.35094400
Mg	-1	-0.07646500	3.92890700	-1.40015500
O	-1	1.90754400	3.97472500	-1.51511400
O	-1	-2.07435400	3.98233500	-1.44892200
O	-1	-6.04080000	3.87684600	-1.33385100
Mg	-1	5.83445700	3.85819400	0.34683300
O	-1	3.92314500	4.04982200	0.58761400
Mg	-1	1.94118600	4.01162100	0.52472600
Mg	-1	-2.02848200	4.02079500	0.59011500
O	-1	-4.00622600	4.06836000	0.73377800
O	-1	-0.04571400	4.09491700	0.64150900
Mg	-1	-5.92597000	3.88928200	0.57189900
C	0	-0.28110800	2.05506600	5.04313700
C	0	0.47064400	1.58612800	3.79850000
C	0	1.62350600	0.63589600	4.02163500
C	0	2.19026900	0.45264400	5.39773400
O	0	2.12144000	0.02263300	3.05938400
H	0	-0.74073900	1.21700800	5.57497100
H	0	0.37286900	2.58589400	5.74030500
H	0	-1.08047000	2.74059000	4.75148100
H	0	0.88837900	2.44933500	3.25598800
H	0	-0.20841300	1.07711500	3.10138000
H	0	3.01239600	-0.26075500	5.36255200
H	0	1.41914400	0.09714900	6.08823200
H	0	2.55076400	1.41168400	5.78589400

1 2 1.0 3 1.0 4 1.0 9 1.0 21 1.0 29 1.0 32 1.0 35 1.0
2 3 1.0 4 1.0 16 1.0 19 1.0 29 1.0 31 1.0 42 1.0
3 9 1.0 16 1.0
4 29 1.0
5 6 1.0 7 1.0 12 1.0 22 1.0 24 1.0 40 1.0 59 1.0 60 1.0 62
1.0 67 1.0
6 7 1.0 13 1.0 15 1.0 24 1.0 25 1.0 27 1.0 28 1.0 50 1.0 55
1.0
7 27 1.0 59 1.0
8 9 1.0 10 1.0 21 1.0 35 1.0 36 1.0 57 1.0 58 1.0 64 1.0
9 10 1.0 11 1.0 16 1.0 21 1.0 23 1.0 35 1.0 51 1.0

10 11 1.0 57 1.0
 11 12 1.0 22 1.0 23 1.0 38 1.0 39 1.0 57 1.0 60 1.0 61 1.0 66
 1.0
 12 22 1.0 38 1.0 60 1.0
 13 14 1.0 15 1.0 17 1.0 18 1.0 20 1.0 22 1.0 24 1.0 43 1.0 48
 1.0
 14 15 1.0 20 1.0 25 1.0 26 1.0 43 1.0 44 1.0 53 1.0
 15 25 1.0
 16 17 1.0 18 1.0 19 1.0 22 1.0 23 1.0 42 1.0 47 1.0
 17 18 1.0 19 1.0 20 1.0 42 1.0 43 1.0 45 1.0 46 1.0
 18 22 1.0
 19 42 1.0
 20 43 1.0
 21 35 1.0
 22 23 1.0 24 1.0 49 1.0 52 1.0
 23
 24 49 1.0
 25 26 1.0 28 1.0 53 1.0 54 1.0 55 1.0
 26 53 1.0
 27 28 1.0 55 1.0 56 1.0 59 1.0 63 1.0 70 1.0
 28 55 1.0
 29 30 1.0 31 1.0 32 1.0
 30 31 1.0 32 1.0 35 1.0 37 1.0 42 1.0 47 1.0 51 1.0
 31 42 1.0
 32 35 1.0
 33 40 1.0 49 1.0 50 1.0 55 1.0 56 1.0 67 1.0 68 1.0 70 1.0
 34 35 1.0 36 1.0 37 1.0 39 1.0 51 1.0 64 1.0 65 1.0 66 1.0
 35 36 1.0 51 1.0
 36 64 1.0
 37 38 1.0 39 1.0 45 1.0 47 1.0 51 1.0 52 1.0
 38 39 1.0 40 1.0 49 1.0 52 1.0 60 1.0 66 1.0 67 1.0 69 1.0
 39 66 1.0
 40 49 1.0 67 1.0
 41 43 1.0 44 1.0 48 1.0 49 1.0 50 1.0 53 1.0 54 1.0 55 1.0
 42 45 1.0 46 1.0 47 1.0
 43 44 1.0 45 1.0 46 1.0 48 1.0
 44 53 1.0
 45 46 1.0 47 1.0 48 1.0 49 1.0 52 1.0
 46
 47
 48 49 1.0
 49 50 1.0 52 1.0
 50 55 1.0
 51
 52
 53 54 1.0
 54 55 1.0
 55 56 1.0
 56 70 1.0
 57 58 1.0 61 1.0 64 1.0 65 1.0 66 1.0
 58 64 1.0
 59 62 1.0 63 1.0 67 1.0 68 1.0 70 1.0
 60 61 1.0 62 1.0 66 1.0 67 1.0 69 1.0

61 66 1.0
62 67 1.0
63 70 1.0
64 65 1.0
65 66 1.0
66 69 1.0
67 68 1.0 69 1.0
68 70 1.0
69
70
71 72 1.0 76 1.0 77 1.0 78 1.0
72 73 1.0 79 1.0 80 1.0
73 74 1.0 75 2.0
74 81 1.0 82 1.0 83 1.0
75
76
77
78
79
80
81
82
83



จุฬาลงกรณ์มหาวิทยาลัย
CHULALONGKORN UNIVERSITY

REFERENCES

1. Wu, L.; Moteki, T.; Gokhale, A. A.; Flaherty, D. W.; Toste, F. D. J. C., Production of fuels and chemicals from biomass: condensation reactions and beyond. **2016**, *1* (1), 32-58.
2. Yutthalekha, T.; Suttipat, D.; Salakhum, S.; Thivasasith, A.; Nokbin, S.; Limtrakul, J.; Wattanakit, C. J. C. C., Aldol condensation of biomass-derived platform molecules over amine-grafted hierarchical FAU-type zeolite nanosheets (Zeolean) featuring basic sites. **2017**, *53* (90), 12185-12188.
3. Alam, M. I.; Gupta, S.; Bohre, A.; Ahmad, E.; Khan, T. S.; Saha, B.; Haider, M. A. J. G. C., Development of 6-amyl- α -pyrone as a potential biomass-derived platform molecule. **2016**, *18* (24), 6431-6435.
4. Hora, L.; Kelbichová, V.; Kikhtyanin, O.; Bortnovskiy, O.; Kubička, D. J. C. T., Aldol condensation of furfural and acetone over MgAl layered double hydroxides and mixed oxides. **2014**, *223*, 138-147.
5. Serrano-Ruiz, J. C.; Luque, R.; Sepúlveda-Escribano, A. J. C. S. R., Transformations of biomass-derived platform molecules: from high added-value chemicals to fuels via aqueous-phase processing. **2011**, *40* (11), 5266-5281.
6. Kikhtyanin, O.; Kelbichová, V.; Vitvarová, D.; Kubů, M.; Kubička, D. J. C. T., Aldol condensation of furfural and acetone on zeolites. **2014**, *227*, 154-162.
7. Liang, G.; Wang, A.; Zhao, X.; Lei, N.; Zhang, T. J. G. C., Selective aldol condensation of biomass-derived levulinic acid and furfural in aqueous-phase over MgO and ZnO. **2016**, *18* (11), 3430-3438.
8. Faba, L.; Díaz, E.; Ordóñez, S. J. A. C. B. E., Aqueous-phase furfural-acetone aldol condensation over basic mixed oxides. **2012**, *113*, 201-211.
9. Zhao, L.; Elechi, N.; Qian, R.; Singh, T. B.; Amarasekara, A. S.; Fan, H.-J. J. T. J. o. P. C. A., Origin of the Regioselectivity in the Aldol Condensation between Hydroxymethylfurfural and Levulinic Acid: A DFT Investigation. **2017**, *121* (9), 1985-1992.
10. Wan, M.; Liang, D.; Wang, L.; Zhang, X.; Yang, D.; Li, G. J. J. o. C., Cycloketone condensation catalyzed by zirconia: Origin of reactant selectivity. **2018**, *361*, 186-192.
11. Mathew, A. K.; Abraham, A.; Mallapureddy, K. K.; Sukumaran, R. K., Lignocellulosic Biorefinery Wastes, or Resources? In *Waste Biorefinery*, Elsevier: 2018; pp 267-297.
12. Mamman, A. S.; Lee, J. M.; Kim, Y. C.; Hwang, I. T.; Park, N. J.; Hwang, Y. K.; Chang, J. S.; Hwang, J. S. J. B., Bioproducts; economy, B. I. f. a. s., Furfural: Hemicellulose/xylo-derived biochemical. **2008**, *2* (5), 438-454.
13. Lange, J. P.; Van Der Heide, E.; van Buijtenen, J.; Price, R. J. C., Furfural—a promising platform for lignocellulosic biofuels. **2012**, *5* (1), 150-166.
14. Dunlop, A. J. I.; Chemistry, E., Furfural formation and behavior. **1948**, *40* (2), 204-209.
15. Yoneda, H.; Tantillo, D. J.; Atsumi, S. J. C., Biological Production of 2-Butanone in *Escherichia coli*. **2014**, *7* (1), 92-95.
16. Chen, Z.; Sun, H.; Huang, J.; Wu, Y.; Liu, D. J. P. o., Metabolic engineering of *Klebsiella pneumoniae* for the production of 2-butanone from glucose. **2015**, *10* (10), e0140508.

17. Guillena, G.; del Carmen Hita, M.; Nájera, C. J. T. A., BINAM-prolinamides as recoverable catalysts in the direct aldol condensation. **2006**, *17* (5), 729-733.
18. Cornforth, J. W. J. A. j. o. c., The trouble with synthesis. **1993**, *46* (2), 157-170.
19. Palomo, C.; Oiarbide, M.; García, J. M. J. C. S. R., Current progress in the asymmetric aldol addition reaction. **2004**, *33* (2), 65-75.
20. Lippert, S.; Baumann, W.; Thomke, K. J. J. o. m. c., Secondary reactions of the base-catalyzed aldol condensation of acetone. **1991**, *69* (2), 199-214.
21. Nielsen, A. T.; Houlihan, W. J. J. O. r., The aldol condensation. **2004**, *16*, 1-438.
22. Carey, F. A.; Sundberg, R. J., *Advanced Organic Chemistry: Part B: Reaction and Synthesis*. Springer Science & Business Media: 2007.
23. Julkapli, N. M.; Bagheri, S. J. R. i. I. C., Magnesium oxide as a heterogeneous catalyst support. **2016**, *36* (1), 1-41.
24. Dovesi, R.; Saunders, V.; Roetti, C.; Orlando, R.; Zicovich-Wilson, C.; Pascale, F.; Civalieri, B.; Doll, K.; Harrison, N.; Bush, I., CRYSTAL17. **2017**.
25. Band, Y. B.; Avishai, Y., *Quantum mechanics with applications to nanotechnology and information science*. Academic Press: 2013.
26. Parr, R. G., Density functional theory of atoms and molecules. In *Horizons of Quantum Chemistry*, Springer: 1980; pp 5-15.
27. Rasmussen, J. J.; Rypdal, K. J. P. S., Blow-up in nonlinear schrodinger equations-i a general review. **1986**, *33* (6), 481.
28. Kaxiras, E., *Atomic and electronic structure of solids*. Cambridge University Press: 2003.
29. Born, M.; Oppenheimer, R. J. A. d. p., Zur quantentheorie der molekeln. **1927**, *389* (20), 457-484.
30. Abdulsattar, M. A. J. J. o. A. P., SiGe superlattice nanocrystal infrared and Raman spectra: A density functional theory study. **2012**, *111* (4), 044306.
31. Sahni, V., The Hohenberg-Kohn Theorems and Kohn-Sham Density Functional Theory. In *Quantal Density Functional Theory*, Springer: 2004; pp 99-123.
32. Zhao, Y.; Truhlar, D. G. J. T. C. A., The M06 suite of density functionals for main group thermochemistry, thermochemical kinetics, noncovalent interactions, excited states, and transition elements: two new functionals and systematic testing of four M06-class functionals and 12 other functionals. **2008**, *120* (1-3), 215-241.
33. Hajek, J.; Vandichel, M.; Van de Voorde, B.; Bueken, B.; De Vos, D.; Waroquier, M.; Van Speybroeck, V., Mechanistic studies of aldol condensations in UiO-66 and UiO-66-NH₂ metal organic frameworks. *Journal of Catalysis* **2015**, *331*, 1-12.
34. Gao, J.; Teplyakov, A. V. J. J. o. c., Chemical transformations of acetone on ZnO powder. **2014**, *319*, 136-141.



จุฬาลงกรณ์มหาวิทยาลัย
CHULALONGKORN UNIVERSITY

VITA

NAME Wilasinee Heebnak

DATE OF BIRTH 9 August 1994

PLACE OF BIRTH Lopburi

**INSTITUTIONS
ATTENDED** 2016 , B.Sc , Thammasat University

HOME ADDRESS 660 Ideo Q Chula-Samyan condo Rama IV Road, Bang-
rak, Bangkok 10500



จุฬาลงกรณ์มหาวิทยาลัย
CHULALONGKORN UNIVERSITY